Variable-Range Hopping Electron Transfer through Disordered Bridge States: Application to DNA

Thomas Renger* and R. A. Marcus

Noyes Laboratory of Chemical Physics, Mail Code 127-72, Pasadena, California 91125

Received: August 19, 2002; In Final Form: July 25, 2003

A theory for electron transfer through a donor−bridge−acceptor system is described that involves tunneling and hopping-like transfers and an intermediate regime. The theory considers how a delocalization of electronic states and static and dynamic disorder in electronic energies influence the charge transfer rate and is used to study experiments on hole transfer through DNA. While an exponential distance dependence of the yield of hole trapping is observed experimentally for small bridges, the yield for long bridges is reported to be almost distance-independent. For long bridge lengths, for which thermally activating hopping dominates over tunneling, the model considers two competing channels, a hopping via localized states and a transfer through partly delocalized states. The variable-range hopping mechanism and the delocalized states aspect of the theory are used to interpret the flat rather than a slow decrease of yield with increasing distance reported in experiments with long bridges.

I. Introduction

In experiments on charge transfer through a DNA π-stack, a wide range of β-values, values which characterize the exponent of the decay of the rate constant with distance, have been measured. In pioneering experiments of the Barton group,[1,2] β values as small as 0.1 $Å^{-1}$ were reported. Similarly small β values were reported by Schuster et al.[3,4] and were discussed in terms of a phonon-assisted polaron hopping model. Other experiments[5−11] yielded larger values up to $\beta = 1.4$ $Å^{-1}$, for example, in Fukui and Tanaka[11] and indicated the superexchange transfer mechanism well-known from electron transfer in proteins.[12]

It was understood from earlier theories[13,14] (see also the recent work in ref 15 and 16) that depending on the energetics of the system studied, either the superexchange mechanism or the hopping mechanism dominate the observed electron/hole transfer, leading to the strong or weak distance dependence of the rate constant, respectively. Numerical calculations applying a Redfield relaxation model were performed[13] on a model donor−bridge−acceptor system. The latter was coupled to one effective high-frequency mode, of which the potential energy minimum was shifted by the reaction. It was found that for large bridge lengths the rate constant becomes weakly dependent on distance and the transfer occurs in a hopping-like mechanism whereas for shorter bridges the tunneling dominates and a strong exponential distance dependence for the rate was obtained. The same result was obtained in theoretical studies performed using a Liouville pathway correlation-function approach.[14,17] The latter included the coupling of the electron to a manifold of vibrational modes and contained the reorganization of a whole set of nuclear coordinates involved in the electron transfer.[14]

Experimental evidence on the critical role of the energetics of the system was provided by Meggers et al.,[9] who demonstrated that the holes for short bridge lengths of adenines (A's) will tunnel through the A's and hop between guanines (G's), an experiment that prompted extensive theoretical analyses.[18−21]

The application of ultrafast time-resolved spectroscopy made it possible to resolve the charge-transfer dynamics in real time. In experiments on an ethidium system,[22] a distance-independent rate was found for hole transfer between a photoexcited ethidium and a deazaguanine for bridges of two, three, and four bases. There was also a decrease of the amplitude of the pump−probe signal for longer bridges, which was explained by static disorder. This finding shed some light on earlier frequency domain experiments[23] on the same system, which had yielded a $\beta \approx 0.1$; the time-domain experiment suggested that this β value does not contain information on the intrinsic distance dependence of the rate constant per se but rather reflects the disorder. Under such conditions, the slow step is not the transmission along the chain of base pairs.

In time-domain experiments on DNA hairpins, an exponential distance dependence of the rate constant of hole transfer between a stilbene and a guanine was found with a $\beta \approx 0.7$.[7,8] A similar β value was obtained in recent time-resolved experiments on an aminopurine (Ap) system[10] for short bridge lengths. The rate constant between Ap and G in $Ap(A)_NG$ became distance-independent for $N > 3$, an indication of a change from superexchange to hopping-like transfer. Bixon and Jortner[24] explained an experiment[25] on hole transfer between guanine triplets in terms of thermally induced hopping.

Recently, in another experiment[26] by the Giese group, experimental evidence for the presence of both transfer mechanisms was obtained in measurements of the distance dependence of the yield of DNA cleavage triggered by hole transfer. As expected, for short bridges ($N < 3$) the superexchange mechanism dominates and the relative yield of DNA cleavage decreases exponentially ($\beta \approx 0.7$) with distance. For bridge lengths $N > 3$, a transition occurs in which the relative yield becomes almost distance-independent. As shown below, the latter observation is not explained simply in terms of thermally activated nearest-neighbor hopping through the bridge. That result served as a stimulus for the present paper, although the

* To whom correspondence should be addressed. Present address: Institut für Chemie (Kristallographie), Freie Universität Berlin, Takustrasse 6, D-14195 Berlin, Germany. E-mail: rth@chemie.fu-berlin.de.

10.1021/jp026789c CCC: $25.00
Published on Web 09/19/2003

theory is intended to be of more general use than just to explain a certain experiment on hole tranfer in DNA.

The present theory combines different aspects of recent[14,27,28] theoretical approaches: The Hamiltonian and the description of the dissipative hole transfer is similar to those used by Okada et al.,[14] though the execution of the theory is different. Whereas Okada et al.[14] used a projection operator technique to obtain the rate, we use simple time-dependent perturbation theory. Also, Okada et al. used a Brownian oscillator model for the description of the electron-vibrational coupling, and here we use a simple harmonic oscillator approach. The Brownian oscillator approach[29] describes dissipation of electronic energy by a damping of the vibrational motion of a few primary harmonic oscillators that couple to the electronic states. The damping results from a coupling between the primary and a large number of bath oscillators. In the harmonic oscillator approach, all oscillators couple directly to the electronic states and dissipation occurs because of destructive interference of the many harmonic modulations of electronic energies. Georgievskii et al.[30] noted that an effective description in terms of harmonic oscillators can be found within an approximate cumulant expansion even for a strongly anharmonic system. If the number of primary oscillators becomes very large and the damping by the bath oscillators becomes zero, the two approaches are formally identical. We use this limit to show the equivalence of the expressions of the rate constant derived here with the earlier result.[14] The present result appears simpler than the earlier one. In the application, we investigate here the effect of static disorder that was not considered in ref 14. Very recently,[27] Berlin et al. gave an explanation of the Giese experiment[26] in terms of a phenomenological model that used a description of the bridge in terms of a tight-binding band. The present treatment includes in addition a description of dynamic and static disorder of this band and yields a phenomenon that has been termed variable-range hopping.[31] Variable-range hopping was applied as a very useful concept by Yu and Song[28] in their treatment of the measured temperature dependence of electrical conductivity in DNA.[32]

The paper is organized as follows. The kinetic scheme is given in section 2 for a charge transfer between a single guanine (G) and three adjacent guanines (GGG) connected by a bridge of adenines (A). An analytical formula for the hopping transfer is derived and examined, taking into account thermal-activated hopping through nearest neighbors in the bridge. The model is used to motivate the need for a more general theory, based on variable-range hopping instead of only nearest-neighbor hopping, which is then formulated. A microscopic rate constant is derived in section 3 for a transition between delocalized electronic states. Account is taken of the local coupling to effective harmonic oscillators, described by a spectral density. The latter is extracted from an independent quantity, the absorption and fluorescence spectra of ethidium intercalated in DNA. The model is applied in section 4 and compared with experimental data[26] on yields for cleavage of DNA. The results are discussed in section 5.

II. Kinetic Scheme and Phenomenological Model for the Giese Experiment

In the experiment of Giese et al.,[26] a single guanine is oxidized following a continuous UV irradiation. The reaction scheme is described in Figure 1, in which the rate constant for hole injection into a guanine is denoted by P. After injection, the hole may be either trapped by an irreversible reaction with water, leading to the product P_G and described by a rate constant k_d,

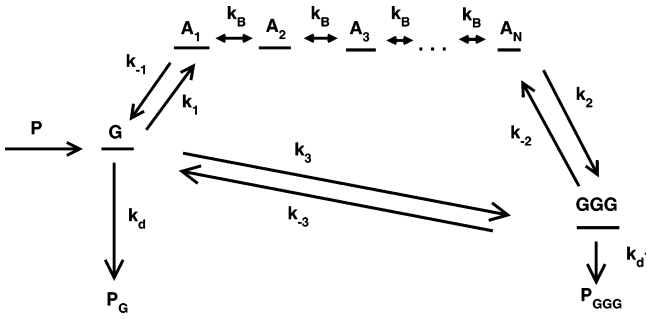

Figure 1. Scheme of hole transfer investigated in Giese's experiment.[26]

or transferred to a sink, GGG, and trapped there with a rate constant k'_d (as noted in ref 9, only about 10% of the injected holes react irreversibly with water and can be detected, whereas the major part of oxidized G and GGG is repaired by deprotonation and subsequent H-abstraction. Therefore, a critical assumption in the interpretation of these types of experiments is that the ratio of the irreversible reaction with water and repair does not depend on the distance between G and GGG). In the experiment, the products P_G and P_{GGG} are measured for different bridge lengths, that is, the number N of intervening A's in $G(A)_N GGG$. The relative yield P_{GGG}/P_G depends on the rate of hole transfer between G and GGG across the N A's. As noted earlier, two distinctly different pathways contribute to this rate constant. The hole may tunnel directly from G to GGG as described in Figure 1 by the rate constant k_3, or thermally activated, it may hop through the bridge, a process that is described in Figure 1 by the rate constants k_1, k_{-1}, k_B, k_2, and k_{-2}. The kinetic equations for the scheme in Figure 1 are given by

$$\frac{dG}{dt} = P(t) - (k_1 + k_3 + k_d)G + k_{-1}A_1 + k_{-3}GGG \quad (1a)$$

$$\frac{dA_1}{dt} = k_1 G - (k_{-1} + k_B)A_1 + k_B A_2 \quad (1b)$$

$$\frac{dA_n}{dt} = k_B A_{n-1} - 2k_B A_n + k_B A_{n+1}, \quad n = 2 \text{ to } (N-1) \quad (1c)$$

$$\frac{dA_N}{dt} = k_B A_{N-1} - (k_B + k_2)A_N + k_{-2}GGG \quad (1d)$$

$$\frac{dGGG}{dt} = k_3 G + k_2 A_N - (k_{-2} + k_{-3} + k'_d)GGG \quad (1e)$$

where $P(t)$ describes the rate of production of G by a pump pulse or by continuous illumination. In the latter case, $P(t) = P_0$ so does not depend on time. When a steady-state is used for the A_n's ($dA_n/dt = 0$), the above scheme becomes

$$\frac{dG}{dt} = P_0 - (k_3 + k_d + k_h^{eff}(N))G + (k_{-3} + k_{-h}^{eff}(N))GGG \quad (2a)$$

$$\frac{dGGG}{dt} = (k_3 + k_h^{eff}(N))G - (k_{-3} + k_{-h}^{eff}(N) + k'_d)GGG \quad (2b)$$

where the effective hopping rate constants, $k_h^{eff}(N)$ and $k_{-h}^{eff}(N)$, are obtained (Appendix A) as

$$k_h^{eff}(N) = k_B \frac{\frac{k_1}{k_{-1}}}{N - 1 + \frac{k_B}{k_{-1}} + \frac{k_B}{k_2}} \quad (3)$$

and

$$k_{-h}^{eff}(N) = k_h^{eff}(N)/K \quad (4)$$

with the equilibrium constant K

$$K = \exp\left(-\frac{\Delta G^0_{G,GGG}}{kT}\right) \quad (5)$$

Here, $\Delta G^0_{G,GGG}$ denotes the standard free energy difference for hole transfer from G to GGG, which in principle could depend on N.

In the experiments of Giese et al.,[26] there was a steady state for G and GGG during the continuous optical excitation generating the hole injection. The relative yield R of products P_{GGG}/P_G in the scheme in Figure 1 is then obtained from eq 2b as

$$R \equiv \frac{P_{GGG}}{P_G} = \frac{k'_d}{k_d}\frac{GGG}{G} = \frac{k'_d}{k_d}\frac{k_3 + k_h^{eff}(N)}{k_{-3} + k_{-h}^{eff}(N) + k'_d} \quad (6)$$

When the trapping rate constant k'_d is small compared to the back transfer rate constant, $k_{-3} + k_{-h}^{eff}(N)$, the above yield reduces to $(k'_d/k_d)/K$, assuming $k_3 = Kk_{-3}$. It then becomes distance-independent if $\Delta G^0_{G,GGG}$ and (k'_d/k_d) do not depend on distance. Such a behavior can be identified by first noting the relative yields R for the smaller bridge lengths N. The back transfer rate constant k_{-3} decreases exponentially with N because superexchange dominates the rate at short distances, and the trapping rate k'_d is expected to be relative insensitive to N. In the experiment of Giese et al.,[26] the rate was not distance-independent at short bridge lengths, so the trapping rate k'_d can be assumed to be larger than the back transfer rate constant, $k_{-3} + k_{-h}^{eff}(N)$, rather than smaller. The relative yield R in this case becomes

$$R = \frac{k_3 + k_h^{eff}(N)}{k_d} \quad (7)$$

We consider next the hopping regime of the transfer, which dominates the transfer rate for $N > 3$ in the experiment of Giese et al.[26] In this case, the superexchange rate constant k_3 in eq 7 can be approximately neglected, and the relative yield R becomes

$$R = \frac{a}{N - 1 + x}, \quad N > 3 \quad (8)$$

where

$$a = (k_B/k_d)(k_1/k_{-1}) \quad x = k_B/k_{-1} + k_B/k_2 \quad (9)$$

A test of eq 8 is given in Figure 2. A fit to the data at $N = 5$ shows how the curve of $R(N)$ vs N satisfies the data for different values of x. It is seen that $x = 5$ gives agreement for intermediate values of N but fails for $N = 16$, whereas $x = 30$ describes the experimental yield for $N = 5$ and $N = 16$ but deviates for the intermediate bridge lengths. Given the smallness of the experimental values for $N > 3$, some caution in the interpretation of the single experimental value at $N = 16$ is necessary. Experimental data in the range $N = 9-15$ would be helpful, as would similar experiments in other laboratories covering the wide range of N. Measurements of other products of the reaction of the G^+ and of the GGG^+ with water would be also particularly desirable (only 10% of the total products are measured).[9] In any event, values $x > 1$ mean that the hopping inside the bridge is faster than hopping from the bridge to G or than hopping from the bridge to GGG or than both, for example, as seen from the definition of x in eq 9. We consider next variable-range hopping as a mechanism for explaining the results in Figure 2. We return to possible other origins of this $x \gg 1$ behavior in the Discussion section.

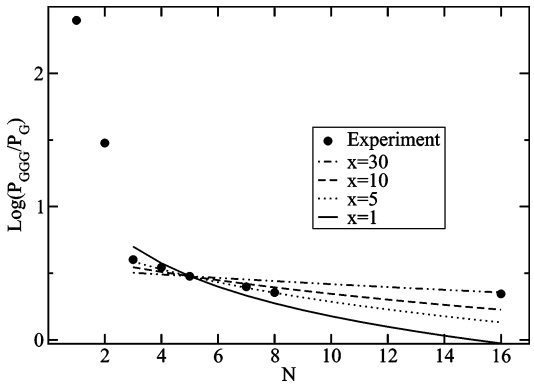

Figure 2. Yields $R = P_{GGG}/P_G$ calculated from eq 8 for $N \geq 3$ for different values x in comparison to experimental values.[26] The parameter a in eq 8 has been chosen to give agreement with the experimental yield for $N = 5$.

III. Theory

A nearest-neighbor tight-binding Hamiltonian[14] used in the following includes the local coupling of electrons and vibrations. The Hamiltonian is expressed in terms of the local hole states, $|i\rangle$, as a basis, where the index i denotes the site at which the hole resides:

$$H = \sum_i E_i(\{Q\})|i\rangle\langle i| + \sum_i V_{i,i+1}(\{Q\})(|i\rangle\langle i+1| + |i+1\rangle\langle i|) + \sum_\xi \frac{\hbar\omega_\xi}{4}(Q_\xi^2 + P_\xi^2) \quad (10)$$

E_i is the local energy of the hole state at site i and $V_{i,i+1}$ is $\langle i|V|i+1\rangle$, where V is an interaction potential. The nuclear environment is described by a set of harmonic oscillators, T_{nucl}, denoting the kinetic energy of the nuclei (e.g., ref 33). Q_ξ and P_ξ are dimensionless nuclear coordinates and momenta related to the spatial coordinates q_ξ and their conjugate momenta p_ξ via $Q_\xi = q_\xi\sqrt{2\mu_\xi\omega_\xi/\hbar}$ and $P_\xi = p_\xi\sqrt{2/(\mu_\xi\omega_\xi\hbar)}$. The mass and frequency for the ξth oscillator are denoted by μ_ξ and ω_ξ, respectively. The electronic energies E_i, as well as the interactions $V_{i,i+1}$, depend on the nuclear coordinates $\{Q\}$. The latter are then related via $Q_\xi = C_\xi^\dagger + C_\xi$ and $P_\xi = i(C_\xi^\dagger - C_\xi)$ to creation and annihilation operator of vibrational quanta.[33]

The energies and couplings are expanded around the equilibrium position of nuclei, defined here as the configuration of nuclei in the absence of a charge carrier. An expansion of up to first-order in Q_ξ yields

$$E_i(\{Q\}) \approx E_i^{(0)} + \sum_\xi \Delta E_i(\xi) Q_\xi$$

$$V_{i,i+1}(\{Q\}) \approx V_{i,i+1}^{(0)} + \sum_\xi \Delta V_{i,i+1}(\xi) Q_\xi \quad (11)$$

The delocalized electronic states $|\mathrm{M}\rangle = \sum_i c_i^{(\mathrm{M})}|i\rangle$ are defined with respect to the equilibrium position of nuclei in the lowest electronic state. The Schrödinger equation is solved,

$$H_0|\mathrm{M}\rangle = \mathscr{E}_\mathrm{M}|\mathrm{M}\rangle \quad (12)$$

where the Hamiltonian H_0 is

$$H_0 = \sum_i E_i^{(0)}|i\rangle\langle i| + \sum_i V_{i,i+1}^{(0)}(|i\rangle\langle i+1| + |i+1\rangle\langle i|) \quad (13)$$

In the proposed eigenstate representation, the Hamiltonian eq 10 becomes

$$H = \sum_\mathrm{M} \mathscr{E}_\mathrm{M}|\mathrm{M}\rangle\langle\mathrm{M}| + \sum_\mathrm{MN}\sum_\xi \hbar\omega_\xi g_\xi(\mathrm{M,N}) Q_\xi |\mathrm{M}\rangle\langle\mathrm{N}| + \sum_\xi \frac{\hbar\omega_\xi}{4}(Q_\xi^2 + P_\xi^2) \quad (14)$$

where the coupling constant $g_\xi(\mathrm{M,N})$ is given in terms of the modulation of electronic energies, $\Delta E_i(\xi)$, and intersite couplings, $\Delta V_{i,i+1}(\xi)$, and the eigencoefficients, $c_j^{(K)}$, of extended states

$$\hbar\omega_\xi g_\xi(\mathrm{M,N}) = \sum_i \Delta E_i(\xi) c_i^{(\mathrm{M})} c_i^{(\mathrm{N})} + \Delta V_{i,i+1}(\xi)(c_i^{(\mathrm{M})} c_{i+1}^{(\mathrm{N})} + c_{i+1}^{(\mathrm{M})} c_i^{(\mathrm{N})}) \quad (15)$$

Next, the potential energy surfaces (PES) for the extended electronic states are constructed by first rewriting the Hamiltonian in eq 14 as

$$H = \sum_\mathrm{M}\left[\mathscr{E}'_\mathrm{M} + \sum_\xi \frac{\hbar\omega_\xi}{4}((Q_\xi + 2g_\xi(\mathrm{M,M}))^2 + P_\xi^2)\right]|\mathrm{M}\rangle\langle\mathrm{M}| + \sum_{\mathrm{MN}}^{\mathrm{M}\neq\mathrm{N}}\sum_\xi \hbar\omega_\xi g_\xi(\mathrm{M,N}) Q_\xi |\mathrm{M}\rangle\langle\mathrm{N}| \quad (16)$$

with the PES minimum at

$$\mathscr{E}'_\mathrm{M} = \mathscr{E}_\mathrm{M} - \lambda_\mathrm{M} \quad (17)$$

where

$$\lambda_\mathrm{M} = \sum_\xi \hbar\omega_\xi g_\xi^2(\mathrm{M,M}) \quad (18)$$

is the solvation energy of the Mth extended electronic state. Until now, both descriptions, the one using local states in eqs 10 and 11 and the one in eq 16, are completely equivalent. However, when rate constants are calculated in the following a critical assumption will be that the nuclei are initially relaxed either in potential energy surfaces of extended states $|\mathrm{M}\rangle$ or in that of local states $|i\rangle$. We consider first the case that the initial relaxation occurs into delocalized electronic states. That is, for a transfer between two different delocalized states M and N, it is assumed that before the transfer occurs the initial extended electronic state M is vibrationally relaxed. The equilibrium position of nuclei for the two states is different because of the coupling to different local vibrational modes and a different degree of electronic delocalization.

A. Rate of Hole Transfer Between Extended Electronic States. A statistical operator $\hat{W}(t)$ is introduced and expanded with respect to the basis $|\mathrm{M}\rangle$ defined in the previous section. The occupation probability P_M of the state $|\mathrm{M}\rangle$ is given as

$$P_\mathrm{M}(t) = \mathrm{tr}_\mathrm{vib}\{\hat{W}(t)|\mathrm{M}\rangle\langle\mathrm{M}|\} = \mathrm{tr}_\mathrm{vib}\{\hat{W}_\mathrm{MM}(t)\} \quad (19)$$

and the trace is over the vibrational degrees of freedom. A perturbation theory second order in the coupling $\hat{V}_\mathrm{MN}$ between different extended states M and N

$$\hat{V}_\mathrm{MN} = \sum_\xi \hbar\omega_\xi g_\xi(\mathrm{M,N}) Q_\xi \quad (20)$$

is used in Appendix B to derive a master equation for the populations $P_\mathrm{M}(t)$:

$$\frac{\mathrm{d}}{\mathrm{d}t}P_\mathrm{M}(t) = -k_{\mathrm{M}\to\mathrm{N}}P_\mathrm{M}(t) + k_{\mathrm{N}\to\mathrm{M}}P_\mathrm{N}(t) \quad (21)$$

where the rate constant $k_{\mathrm{M}\to\mathrm{N}}$ is

$$k_{\mathrm{M}\to\mathrm{N}} = \frac{1}{\hbar^2}\int_{-\infty}^{\infty} \mathrm{d}t\, \mathrm{e}^{i\omega_\mathrm{MN}t}\, \mathrm{tr}_\mathrm{vib}\{U_\mathrm{M}^\dagger(t)\hat{V}_\mathrm{MN}U_\mathrm{N}(t)\hat{V}_\mathrm{NM}W_\mathrm{eq}(\mathrm{M})\} \quad (22)$$

The $\hbar\omega_\mathrm{MN}$ in eq 22 denotes an energy difference between two vibrationally relaxed delocalized electronic states (eq 17)

$$\omega_\mathrm{MN} = \frac{\mathscr{E}'_\mathrm{M} - \mathscr{E}'_\mathrm{N}}{\hbar} \quad (23)$$

$W_\mathrm{eq}(\mathrm{M})$ is the equilibrium statistical operator of the vibrations in the Mth PES, and $U_\mathrm{M}(t)$ is the time-evolution operator of the Mth PES

$$W_\mathrm{eq}(\mathrm{M}) = \mathrm{e}^{-H_\mathrm{vib}(\mathrm{M})/(kT)} \quad (24)$$

$$U_\mathrm{M}(t) = \mathrm{e}^{-iH_\mathrm{vib}(\mathrm{M})t/\hbar} \quad (25)$$

with

$$H_\mathrm{vib}(\mathrm{M}) = \sum_\xi \frac{\hbar\omega_\xi}{4}((Q_\xi + 2g_\xi(\mathrm{M,M}))^2 + P_\xi^2) \quad (26)$$

The rate constant $k_{\mathrm{M}\to\mathrm{N}}$ in eq 22 obeys detailed balance,

$$\frac{k_{\mathrm{M}\to\mathrm{N}}}{k_{\mathrm{N}\to\mathrm{M}}} = \mathrm{e}^{\hbar\omega_\mathrm{MN}/(kT)} \quad (27)$$

(This relation can be obtained by substituting t by $-t - (i\hbar/(kT))$ in eq 22, a substitution, which corresponds to an interchange of the symbols M and N.)

Because harmonic PES are assumed, the rate constant $k_{\mathrm{M}\to\mathrm{N}}$ in eq 22 can be calculated without further approximation. The new result, obtained in Appendix B, is

$$k_{\mathrm{M}\to\mathrm{N}} = \int_{-\infty}^{\infty} \mathrm{d}\tau\, \mathrm{e}^{i\omega_\mathrm{MN}\tau}\, \mathrm{e}^{\phi_\mathrm{MN}(\tau)-\phi_\mathrm{MN}(0)}\left[\left(\frac{\lambda_\mathrm{MN}}{\hbar} + G_\mathrm{MN}(\tau)\right)^2 + F_\mathrm{MN}(\tau)\right] \quad (28)$$

where the time-dependent functions

$$\phi_{MN}(t) = \sum_i (|c_i^{(M)}|^2 - |c_i^{(N)}|^2)^2 \phi_0(t) \quad (29)$$

$$G_{MN}(t) = \sum_i ((c_i^{(M)})^3 c_i^{(N)} - (c_i^{(N)})^3 c_i^{(M)}) \phi_1(t) \quad (30)$$

$$F_{MN}(t) = \sum_i |c_i^{(M)}|^2 |c_i^{(N)}|^2 \phi_2(t) \quad (31)$$

were introduced with

$$\phi_n(t) = \int_{-\infty}^{\infty} d\omega\, e^{-i\omega t} (1 + n(\omega)) \omega^n (J(\omega) - J(-\omega)) \quad (32)$$

The preceding function contains the mean number $n(\omega)$ of vibrational quanta of energy, $\hbar\omega$, at temperature T,

$$n(\omega) = (\exp\{\hbar\omega/(kT)\} - 1)^{-1} \quad (33)$$

and a spectral density, $J(\omega)$,

$$J(\omega) = \sum_\xi \left(\frac{\Delta E(\xi)}{\hbar\omega_\xi}\right)^2 \delta(\omega - \omega_\xi) \quad (34)$$

characterizing the fluctuations of local hole energies. The same spectral density will be assumed for all sites, and the correlation between fluctuations at different sites and any fluctuations of electronic couplings will be neglected. The time-independent part in the integrand in eq 28, λ_{MN}, is

$$\lambda_{MN} = \sum_i [(c_i^{(M)})^3 c_i^{(N)} + (c_i^{(N)})^3 c_i^{(M)}] E_\lambda \quad (35)$$

where a reorganization energy E_λ is introduced as[33]

$$E_\lambda = \int d\omega\, \hbar\omega J(\omega) \quad (36)$$

The solvation reorganization energy λ_M of extended state M in eq 18, using the above approximations, then becomes

$$\lambda_M = E_\lambda L_M^{-1} \quad \text{with} \quad L_M^{-1} = \sum_i |c_M^{(i)}|^4 \quad (37)$$

where L_M^{-1} is the so-called inverse participation ratio[34] that is a measure for the delocalization of state M. It can vary between 1 for localized states and N^{-1} for completely delocalized states, where N is the number of coupled sites. Herein, the standard result for the rate constant between localized states will be given first, and in the Discussion section, an interpretation of the present result in eqs 28−37 is given in terms of a comparison with the rate constant for localized states.

B. Rate of Hole Transfer between Local Electronic States. To recover from the Hamiltonian in eq 10, the usual expression for the nonadiabatic electron transfer between localized states this Hamiltonian is rewritten as

$$H = \sum_i \left[E_i' + \sum_\xi \frac{\hbar\omega_\xi}{4}((Q_\xi + 2g_\xi(i))^2 + P_\xi^2)\right] |i\rangle\langle i| + \sum_i V_{i,i+1}(|i\rangle\langle i+1| + |i+1\rangle\langle i|) \quad (38)$$

where eq 11 was used for the modulation of electronic energies and where the modulation of the couplings was neglected as before, that is, $V_{i,i+1} = V_{i,i+1}^{(0)}$. The modulation of energies, $\Delta E_i(\xi)$, is contained in the coupling constant $g_\xi(i)$ at site i,

$$g_\xi(i) = \frac{\Delta E_i(\xi)}{\hbar\omega_\xi} \quad (39)$$

using the $\Delta E_i(\xi)$ in eq 11. The energies E_i', namely, the energies of the localized states, are

$$E_i' = E_i - \sum_\xi \hbar\omega_\xi (g_\xi(i))^2 \quad (40)$$

The rate constant $k_{i\to j}$ for hole transfer between states of the system where the hole is localized at sites i and j then follows as

$$k_{i\to j} = \frac{|V_{i,j}|^2}{\hbar^2} \int_{-\infty}^{\infty} dt\, e^{i\omega_{ij}t}\, \mathrm{tr}_{vib}\{U_i^\dagger(t) U_j(t) W_{eq}(i)\} \quad (41)$$

where $\omega_{ij} = (E_i' - E_j')/\hbar$ is given in terms of the energies in eq 40 and $U_i(t)$ is the time-evolution operator of the vibrations in the PES of the state with a localized hole at site i (that PES is called the ith PES in the following).

$$U_i(t) = e^{-iH_{vib}(i)t/\hbar} \quad (42)$$

where

$$H_{vib}(i) = \sum_\xi \frac{\hbar\omega_\xi}{4}((Q_\xi + 2g_\xi(i))^2 + P_\xi^2) \quad (43)$$

The equilibrium statistical operator of the vibrations in the ith PES is $W_{eq}(i)$:

$$W_{eq}(i) = e^{-H_{vib}(i)/(kT)} \quad (44)$$

The rate constant $k_{i\to j}$ in eq 41 for transfer between localized states can be calculated in a manner similar to that used for the delocalized states in Appendix B. The calculation is simplified by the fact that the coupling between different states does not depend on the coordinates, in contrast with Appendix B. The well-known result for nonadiabatic electron transfer between localized states is[33,35−37]

$$k_{i\to j} = \frac{|V_{i,j}|^2}{\hbar^2} \int_{-\infty}^{\infty} dt\, e^{i\omega_{ij}t}\, e^{\phi(t) - \phi(0)} \quad (45)$$

where the time-dependent function is

$$\phi(t) = \int_{-\infty}^{\infty} d\omega\, e^{-i\omega t} (1 + n(\omega))(J_{ij}(\omega) - J_{ij}(-\omega)) \quad (46)$$

with the spectral density

$$J_{ij}(\omega) = \sum_\xi (g_\xi(i) - g_\xi(j))^2 \delta(\omega - \omega_\xi) \quad (47)$$

which is zero for negative ω. When the fluctuations of energies at sites i and j are not correlated, this spectral density becomes

$$J_{ij}(\omega) = J_i(\omega) + J_j(\omega) = 2J(\omega) \quad (48)$$

where the local spectral density, given in eq 34, was also assumed here. The $\phi(t)$ in eq 46 then equals $2\phi_0(t)$ in eq 32.

The well-known classical limit of the rate constant in eq 45 is[33,35,36]

$$k_{i\to j} = \frac{2\pi}{\hbar}\frac{|V_{i,j}|^2}{\sqrt{4\pi\lambda kT}}\,\mathrm{e}^{-(\lambda-\hbar\omega_{ij})^2/(4\lambda kT)} \tag{49}$$

where the reorganization energy λ[38] is related to the local reorganization energy in eq 36 by

$$\lambda = 2E_\lambda \tag{50}$$

and the standard free energy of the reaction is $\Delta G^\circ_{ij} = -\hbar\omega_{ij}$.

IV. Numerical Calculation of Hole Transfer

A. Estimate of the Spectral Density from Optical Spectra and Normal-Mode Analysis. In the following, a rough estimate of the spectral density $J(\omega)$ in eq 34 is obtained from the calculation of absorption and fluorescence spectra of a dye molecule intercalated in DNA. Although the $J(\omega)$ in eq 34 is a spectral density for charge transfer and the $J(\omega)$ extracted in the following is an optical spectral density, the latter is an approximation for the former as discussed in detail in the Discussion section.

The optical line shapes of absorption, D_α, and fluorescence, D_I, then are related to the spectral density in eq 34 according to[33,37,39]

$$D_{\alpha,I}(\omega) \approx \mathrm{e}^{-\phi_0(0)}(2\pi\delta(\omega-\omega_{10}) + \int_{-\infty}^{\infty}\mathrm{d}t\,\mathrm{e}^{\pm\imath(\omega-\omega_{10})t}\{\mathrm{e}^{\phi_0(t)}-1\}) \tag{51}$$

where the function $\phi_0(t)$ in eq 32 was used and $\hbar\omega_{10}$ is the energy difference between the minima of the potential energy surfaces of the ground and excited state of the dye. As seen in eq 34, the spectral density is given as a combination of coupling factors and density of states. The density of states

$$d(\omega) = \sum_\xi \delta(\omega-\omega_\xi) \tag{52}$$

of a DNA fragment with intercalated ethidium was calculated from a normal-mode analysis in ref 40. For the local spectral density $J(\omega)$, the following ansatz is chosen:

$$J(\omega) = S\kappa(\omega)d(\omega) \tag{53}$$

with

$$\kappa(\omega) = \frac{1}{\omega_c}\,\mathrm{e}^{-\omega/\omega_c} \tag{54}$$

and the well-known Huang−Rhys factor

$$S = \int \mathrm{d}\omega\, J(\omega) \tag{55}$$

A frequency ω_c was introduced in eq 54 to take cognizance of the fact that the high-frequency normal modes are typically more localized than the low-frequency modes and therefore only few of the former belong to the local site where the ethidium is intercalated and thus couple to its optical transition. In addition, $\kappa(\omega)$ takes into account the difference in coupling constants for the different normal modes. The selected functional form is a major simplification in that it limits the number of adjustable parameters to two, namely, the amplitude of the coupling S and the cutoff frequency ω_c. The absorption and fluorescence spectra obtained for $S = 8$ and $\hbar\omega_c = 300\ \mathrm{cm}^{-1}$ are compared in Figure 3 to the experimental values.[41] From the spectral density so-obtained, a local reorganization energy $E_\lambda = 0.24$ eV is calculated from eq 36. The reorganization energy λ for hole transfer between two localized states then is obtained from eq 50 as $\lambda = 0.48$ eV.

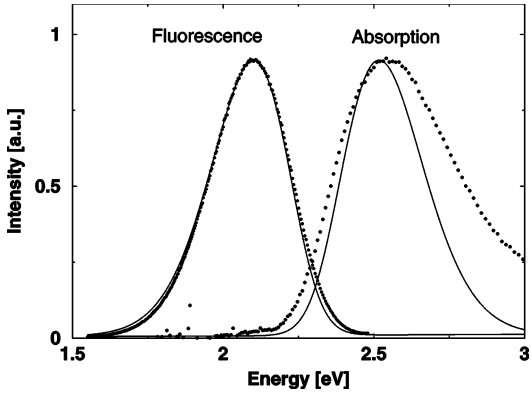

Figure 3. Room-temperature absorption and fluorescence spectra of ethidium bromide intercalated in DNA. Circles are the experimental data,[41] and lines show the calculations.

The deviations between the theoretical and experimental absorption curves in the blue wing of the spectrum can be attributed to the vibrational frequencies being different for the ground and excited state or to higher excited electronic states. The latter are seen in the absorption spectrum but not in fluorescence (because of relaxation to the lowest excited state). There is support for the latter proposition from early quantum chemical studies.[42]

B. Calculation of Experimental Cleavage Yields. Assuming steady-state conditions as before, the following set of equations is next solved for the populations of extended states

$$\sum_N (k_{M\to N} + k_d^{(M)})P_M - \sum_N k_{N\to M}P_N = P_0^{(M)} \tag{56}$$

where $P_0^{(M)}$ describes the rate of production of M by the local hole injection P_0 (production of G),

$$P_0^{(M)} = (c_G^{(M)})^2 P_0 \tag{57}$$

The trapping rate constant $k_d^{(M)}$ in eq 56 for a given extended state M includes the contributions from the G and the GGG state to this extended state

$$k_d^{(M)} = \{(c_G^{(M)})^2 + (c_{GGG}^{(M)})^2\}k_d \tag{58}$$

where we assumed $k_d = k_d'$ for simplicity, that is, the same local trapping rate at G and GGG. There is at present no direct information on the trapping rates available in the literature. An analysis of hole-hopping data on a similar system in ref 21 gave a ratio $k_d/k_d' = 1.6$. Considering the uncertainties of other parameters, this small difference in trapping rates, if real, does not need to be taken into account in our present approximate treatment.

The measured yield, R, is then obtained from the resulting occupation probabilities, P_M, and eigencoefficients, $c_i^{(M)}$

$$R = \frac{\langle P_{GGG}\rangle_{dis}}{\langle P_G\rangle_{dis}} = \frac{\langle\sum_M (c_{GGG}^{(M)})^2 P_M\rangle_{dis}}{\langle\sum_M (c_G)^2 P_M\rangle_{dis}} \tag{59}$$

where $\langle ...\rangle_{dis}$ denotes an average over disorder. The latter is described as a static fluctuation in site energies. A Gaussian distribution function of fwhm Δ_{dis} is assumed independent of

the site index, and the energies at different sites are assumed to vary in an uncorrelated manner. The same mean site energy E_A is assumed for all A's. From the spectral density $J(\omega)$ obtained as described earlier, the functions $\phi_n(t)$ were calculated according to eq 32. Those functions were then used to calculate the functions $F_{MN}(t)$, $\phi_{MN}(t)$, and $G_{MN}(t)$, eqs 29−31, which enter the rate constant expression in eq 28. Each disorder average in eq 59 was performed numerically using a Monte Carlo algorithm. The numerical procedure used to obtain the relative yield consists of the following steps: (i) random generation of site energies from Gaussian distribution functions that are centered around the mean site energies E_A, E_G, and E_{GGG}, (ii) calculation of extended states by diagonalization,[43] (iii) calculation of rate constants, (iv) solution of linear equations for the population of extended states and calculation of populations for G and GGG sites, (v) repetition of steps i−iv for about 10 000 configurations of disorder and calculation of average population of G and GGG sites and the relative yield R.

In addition to the delocalized states channel, a hopping channel through localized states is investigated. When a localized state description is used, the master equations are

$$(k_{i\rightarrow i+1} + k_{i\rightarrow i-1} + (\delta_{i,GGG} + \delta_{i,G})k_d)P_i - k_{i+1\rightarrow i}P_{i+1} - k_{i-1\rightarrow i}P_{i-1} = \delta_{i,G}P_0 \quad (60)$$

where the rate constants $k_{i\rightarrow i+1}$ are calculated from eq 49 using the same parameters as in the extended states calculations. The yield R averaged over disorder is given by

$$R = \frac{\langle P_{GGG}\rangle_{dis}}{\langle P_G\rangle_{dis}} \quad (61)$$

where the disorder average was calculated numerically by a Monte Carlo algorithm as before. In our calculations, the two thermally activated hopping rates, via localized and delocalized states, are treated as independent channels. In this case, the overall yield is just the sum of the two individual yields. However, as will be shown below, it is possible that one channel dominates the yield. Our primary focus is on the thermally activated hopping part of the signal observed for $N > 3$. In this case, both channels are related by an equilibrium constant and the dominant channel is the one for which the product of thermal activation and intrachannel transfer between the respective (localized or delocalized) states is larger.

Besides the spectral density, $J(\omega)$, estimated above, a number of other quantities are needed for the calculations: (i) the electronic couplings, $V_{i,i+1}$, (ii and iii) the energy gaps, ΔE_{AG} and $\Delta E_{G,GGG}$, of the local hole states, (iv) the trapping rate, k_d, and (v) the amount of disorder described by the width (fwhm), Δ_{dis}, of the Gaussian distribution function assumed for the local hole energies. The quantities i and iv were estimated from independent theoretical calculations,[18,44,45] an upper limit for quantity v was obtained from an independent calculation,[28] a lower value for quantity iii was obtained from the present calculation, and quantity ii was fitted to the present experiment. The details are as follows:

Two different sets of electronic matrix elements are reported in the literature.[44,45] In ref 45, the coupling between neighboring A's was calculated to range between 0.125 and 0.198 eV.[46] For the interstrand coupling between A and G and A and GGG, 1 order of magnitude smaller couplings ranging between 0.011 and 0.076 eV were obtained.[45] In contrast to these results, a 1 order of magnitude smaller coupling between A's was obtained in ref 44; the intrastrand A−G and A−GGG couplings are similar in both references. The calculations in Figure 4 refer to the couplings of ref 45; we used 0.165 eV for the intrastrand coupling between A's and 0.03 eV for the interstrand coupling between A and G and A and GGG. The second set of couplings[44] is investigated later.

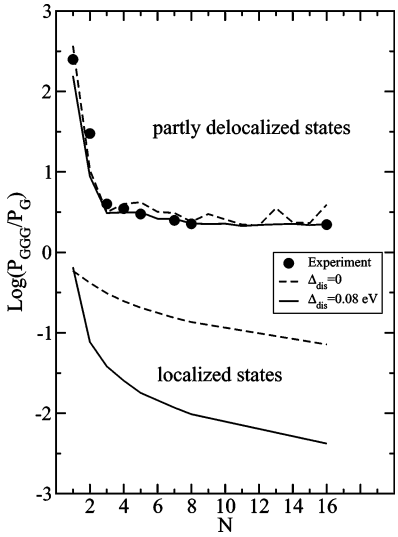

Figure 4. Calculation of relative yields of DNA strand cleavage in dependence on bridge length N for the electronic couplings of Troisi et al.[45] Circles are the experimental values of Giese et al.[26] The upper and lower curves are obtained for the two channels, involving partly delocalized and localized states, respectively. The calculations of solid lines include static disorder, whereas the dashed curves were obtained without taking into account static disorder.

For item iv, the trapping rate k_d, a value of $\sim 10^8$ s^{-1} was estimated earlier from an analysis of a relative yield of hole trapping measured on a similar system.[18] From the calculations, we obtain 7×10^8 s^{-1} for k_d. This value does not influence the shape of the yield versus distance plot; as long as the trapping is fast compared to the back transfer from GGG to G, it just shifts the whole curve along the yield axis.

Item ii, the energy gap ΔE_{AG}, was extracted from the yield, measured in the present experiment for short bridge lengths where superexchange dominates: An energy gap of $\Delta E_{AG} = 0.27$ eV gave the observed slope of the yield versus distance curve in this region and also gave a transition between superexchange and hopping at about $N = 3$, as observed in experiment. This value for ΔE_{AG} lies between the difference in ionization potentials for A and G measured in the gas phase[47] (0.2 eV) and in acetonitrite solution[48] (0.47 eV).

The question of the effect of disorder, Δ_{dis}, in site energies arises. Without use of disorder but with use of extended states, a qualitative fit to the data was obtained (upper part of Figure 4). However, the yield for long bridges shows some nonmonotonical behavior that is not observed in the experiment. This behavior is averaged out in the calculation that takes into account static disorder; a $\Delta_{dis} = 0.08$ eV (fwhm of Gaussian distribution function) was used (Figure 4). We compare this result later with one by Yu and Song[28] obtained from the temperature dependence of conduction.

The yields obtained for a localized states model shown in the lower part of Figure 4 are smaller by 1−2 orders of magnitude than the delocalized states yields. Obviously, the delocalized states hopping channel dominates the transfer for this set of electronic couplings.[45] It is seen also that disorder decreases the localized states yield, an effect discussed in detail later. In addition, the localized states yield shows a stronger distance dependence for long bridge lengths in disagreement with the experimental data.

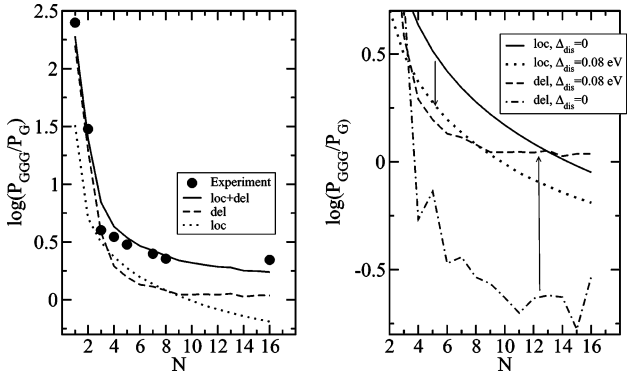

Figure 5. Calculation of relative yields of DNA strand cleavage for the electronic couplings of Voityuk et al.[45] Circles are the experimental values of Giese et al.[26] The solid line in the left part is the logarithm of the sum of the yields obtained for localized states and those obtained for delocalized states. The separate yields are shown in the left part as dashed (for delocalized states channel) and dotted (localized states) lines. A static disorder of $\Delta_{dis} = 0.08$ eV was assumed. The latter two curves are shown again in the right part and are compared there with calculations neglecting disorder.

Next, we consider the second set of electronic couplings from the recent literature,[44] which results in the calculated yields shown in Figure 5. Because of the smaller electronic couplings in the bridge, now both localized and delocalized states contribute to the yield. An electronic matrix element of 0.03 eV for hole transfer between A's was calculated by an ab initio method in ref 44. A similar value (0.02 eV) was obtained[44] for the interstrand coupling of G and A. For simplicity, we used the same coupling $V_{i,i+1} = 0.03$ eV between all bases. For item iv, the trapping rate k_d, we used 1.3×10^8 s^{-1}, which is close to the $\sim 10^8$ s^{-1} estimated earlier.[18]

For item ii, the energy gap ΔE_{AG} was extracted from the yield as before; a $\Delta E_{AG} = 0.14$ eV[49] gave the observed slope of the yield versus distance curve in this region and also gave a transition between superexchange and hopping at about $N = 3$, as observed in experiment. Without use of disorder but with use of extended states, a fit to the data was not obtained. To fit the experiment, a $\Delta_{dis} = 0.08$ eV (fwhm of Gaussian distribution function) was used (Figure 5) as before in Figure 4. The transition between the tunneling and the hopping regime is somewhat smoother ($N = 4$, ..., 8) in the absence of disorder, while in the presence of disorder a sharp transition is obtained at $N = 3$ as apparently observed in the experiment. By comparing the solid with the dashed line and the dot−dashed with the dotted line in the right part of Figure 5, one sees that disorder in site energies decreases the localized states hopping rate and enhances the delocalized states hopping, a result discussed later.

In the calculations in Figures 4 and 5, the energetic difference $\Delta E_{G,GGG} = 0.2$ eV was also assumed.[50] However, the calculated yield does not depend on $\Delta E_{G,GGG}$ as long as this energy gap is large enough to prevent the back transfer $(GGG)^+ + G \rightarrow GGG + G^+$ from being faster than the trapping (rate constant k_d). For smaller energy gaps, the calculated yields for short bridges become independent of distance, in disagreement with the experimental observation.[26] As discussed earlier, the rapid transfer rate constant $k_{GGG\rightarrow G}$ obtained in the calculation for small energy gaps $\Delta E_{G,GGG}$ allows the system to equilibrate before the trapping can occur and leads to this discrepancy for small $\Delta E_{G,GGG}$.

V. Discussion

A. Theoretical Aspects. We consider first a phenomenological nearest-neighbor hopping model, and its use to obtain an effective hopping rate in eq 3 between a donor and an acceptor. The latter are connected by a bridge with hole orbital energies in the bridge being higher than those of the donor and the acceptor. The distance dependence obtained for the rate allows one to estimate a certain ratio of rate constants of the individual transfer processes by comparison with experiment. A density matrix study[51] on activated conduction in molecular junctions gave an $(\alpha_1 + \alpha_2 N)^{-1}$ dependence of the numerically obtained rate, where the constants α_1 and α_2 depend on the molecular properties and on the strength of electron-vibrational coupling. The same distance dependence of the effective rate is obtained here, and the two constants are related to the individual rate constants of the present phenomenological model as $\alpha_1^{-1} = k_{-1} + k_2 - k_B$ and $\alpha_2^{-1} = k_B$. In a recent paper[24] on thermally induced hopping, an N^{-2} dependence of the effective transfer rate was inferred in the limit of $k_B/k_2 \ll 1$. The present result gives, instead, an $(N - 1 + k_B/k_{-1})^{-1}$ distance dependence in this limit.[52]

The more general theory, more general in the sense of being more microscopic, that was used to obtain a rate constant in eq 28 for hole transfer between partly delocalized states is related to an earlier theory due to Mukamel and co-workers.[14,53,54] They describe charge transfer in DNA[14] and exciton transfer in photosynthetic systems.[53,54] The present theory is simpler because it assumes fast vibrational relaxation. The latter assumption leads to the reduction of the entire set of equations for the dynamic variables to master equations. However, the part of the earlier theory[14] that describes the transfer between different electronic states was treated in the Markov approximation, and hence, a similar expression for the rate constant is obtained. The results for the rate constants nevertheless at first glance appear to be quite different from the present ones because of the use of the Brownian oscillator approach for the coupling to vibrations in ref 14. In the present paper, a harmonic oscillator approach is used. The equality of the two rate constants is shown in Appendix C.

The introduction of the PES of the extended electronic states takes into account the dependence of the configuration of nuclei on the delocalization of the electronic state. It is seen in the following section that, as expected, electronic delocalization leads to smaller reorganization energies of charge transfer. Disorder in energies tends to localize the electronic states. Here, localization due to static disorder was taken into account and dynamic localization, the so-called self-trapping,[55,56] was neglected.

Self-trapping of electronic states could be included in the theory by a higher-order perturbation theory in the off-diagonal part of the coupling of extended states to the vibrations. The use of second-order perturbation theory for the off-diagonal parts of the electron-vibrational coupling relies on the assumption that the off-diagonal part, $g_\xi(M,N)$, is smaller than the diagonal part, $g_\xi(M,M)$. The $g_\xi(M,M)$ is taken into account exactly. This relation is a result of static disorder. For completely localized states, the $g_\xi(M,N) = \sum_i c_i^{(M)} c_i^{(N)} g_\xi(i)$ would be zero for $M \neq N$ because one of the two coefficients, $c_i^{(M)}$ or $c_i^{(N)}$, would vanish for $M \neq N$. Instead of taking into account the self-trapping explicitly, we consider two competing channels of thermally activated hopping through partly delocalized states and through localized states as is discussed in detail in section 5.3.

In the present formulation, we have not included a possible dependence of the reorganization energy λ on distance between hopping sites.[57] We expect that a distance dependence will mainly have an influence on the yield for short bridge lengths where tunneling dominates. However, our focus here is on the

thermally activated hopping observed for longer bridges. In the case of nearest-neighbor hopping, there is just a single λ, and in the case of variable-range hopping, it can be expected that an effective λ can be introduced that takes into account an average over different distances.

B. Comparison of Rate Constants for Extended and Localized States. The three major differences between the rate constants for transfer between extended and localized states occur in (i) the free energy difference, (ii) the different displacement of free energy curves, and (iii) the presence of inelastic tunneling processes. The free energy difference, $\hbar\omega_{MN}$, between the extended states M and N in eq 23, using eqs 17 and 18, is

$$\hbar\omega_{MN} = \mathcal{O}_M - \mathcal{O}_N + E_\lambda(L_M^{-1} - L_N^{-1}), \qquad (62)$$

It is seen to depend on the difference in the inverse participation ratio (the delocalization) of extended states M and N. If the states M and N are localized at sites i and j, respectively, then $\hbar\omega_{MN} = \hbar\omega_{ij}$ using $L_M^{-1} = L_N^{-1} = 1$.

To illustrate the points ii and iii, it is assumed, for simplicity, that every site couples to only one local vibrational mode with frequency ω_0. The spectral density in eq 34 in this case reduces to

$$J(\omega) = g_0^{\,2}\delta(\omega - \omega_0) \qquad (63)$$

where $g_0 = \Delta E/(\hbar\omega_0)$, and the function $\phi_n(t)$ in eq 32 now becomes

$$\phi_n(t) = g^2\omega_0^{\,n}(e^{-i\omega_0 t}(1 + n(\omega_0)) + e^{i\omega_0 t}n(\omega_0)) \qquad (64)$$

The function $e^{\phi_{MN}(\tau)}$ in eq 28 then can be expanded as

$$e^{\phi_{MN}(\tau)} = \sum_{k=0}^{\infty}\sum_{l=0}^{\infty}\frac{(\Delta_{MN}g_0^{\,2})^{k+l}}{k!l!}e^{-i(k-l)\omega_0\tau}(1 + n(\omega_0))^k(n(\omega_0))^l \qquad (65)$$

with

$$\Delta_{MN} = \sum_i(|c_i^{(M)}|^2 - |c_i^{(N)}|^2)^2 \qquad (66)$$

The extended state rate constant in eq 28 then can be written as

$$\begin{aligned} k_{M\to N} = \sum_{k,l=0}^{\infty} & P_i(l,y{=}\Delta_{MN})P_f(k,y{=}\Delta_{MN}) \times \\ & (\{(\lambda_{MN}/\hbar)^2 - 2A_2(1 + n(\omega_0))n(\omega_0)\}\delta(\omega_{MN} - \omega_0(k - l)) + \\ & A_{+1}(1 + n(\omega_0))\delta(\omega_{MN} - \omega_0(k + 1 - l)) + \\ & A_{-1}n(\omega_0)\delta(\omega_{MN} - \omega_0(k - l - 1)) + \\ & A_2\{(1 + n(\omega_0))^2\delta(\omega_{MN} - \omega_0(k + 2 - l)) + \\ & n(\omega_0)^2\delta(\omega_{MN} - \omega_0(k - l - 2))\}) \end{aligned} \qquad (67)$$

with the two Poisson distributions

$$P_i(l,y) = e^{-yg_0^2n(\omega_0)}\frac{[yg_0^{\,2}n(\omega_0)]^l}{l!} \qquad (68)$$

and

$$P_f(k,y) = e^{-yg_0^2(1+n(\omega_0))}\frac{[yg_0^{\,2}(1 + n(\omega_0))]^k}{k!} \qquad (69)$$

The constants A_0, $A_{\pm1}$, and A_2 in eq 67 are obtained from $\Delta_1(M,N) = \sum_i((c_i^{(M)})^3c_i^{(N)} - (c_i^{(N)})^3c_i^{(M)})$, $a = 2\lambda_{MN}\omega_0g_0^2\Delta_1(M,N)/\hbar$, and $b = \omega_0^2g_0^2\sum_i|c_i^{(M)}|^2|c_i^{(N)}|^2$ because $A_{+1} = (a + b)$, $A_{-1} = (b - a)$, and $A_2 = \Delta_1(M,N)^2\omega_0^2g_0^4$.

With the use of the same single local vibrational mode approximation and a similar expansion, the rate constant $k_{i\to j}$ between local states in eq 45 is

$$k_{i\to j} = \frac{|V_{i,j}|^2}{\hbar^2}\sum_{k,l=0}^{\infty}P_i(l,y{=}2)P_f(k,y{=}2)\delta(\omega_{ij} - \omega_0(k - l)) \qquad (70)$$

The δ-functions on the rhs of eqs 67 and 70 describe energy conservation during the charge transfer. The transfer occurs between the lth vibrational state of the initial electronic state and the kth vibrational state of the final electronic state.

The two Poisson distributions, eqs 68 and 69, determine the contribution of the vibrational states k and l to the transfer. The maxima of those distributions occur at $l \approx yg_0^2n(\omega_0)$ and $k \approx yg_0^2(1 + n(\omega_0))$. For example, if the two free energy surfaces are strongly displaced (i.e., yg_0^2 is large), those distribution functions are large for large numbers k and l because a large number of vibrational quanta are necessary for sufficiently strong vibrational overlap and energy conservation.

The factor $P_i(l,y{=}\Delta_{MN})P_f(k,y{=}\Delta_{MN})$ in eq 67 depends on the function $y = \Delta_{MN}$ in eq 66. The latter depends on the delocalization of electronic states; it varies between 0 for completely delocalized electronic states (the probabilities $|c_i^{(M)}|^2$ and $|c_i^{(N)}|^2$ to find a local hole state i in the extended states M and N are equal) and 2 for completely localized states (a local hole state i will contribute to either extended state M or extended state N). In the latter case, the factor $P_i(l,y{=}2)P_f(k,y{=}2)$ in eq 70 for localized electronic states is recovered. The Poisson distributions for the localized states peak at higher values of k and l than the distribution functions for extended states, reflecting the fact that a delocalization of electronic states leads effectively to a smaller horizontal displacement of the free energy surfaces of the different states and hence to a smaller reorganization energy of the reaction.

The third difference between eqs 67 and 70 is the appearance of non-Condon terms in the extended state rate constant. Those terms, which appear in eq 67 after the coefficients $A_{\pm1}$ and A_2, result from the coordinate dependence of the coupling (eq 16) between the extended states M and N and describe an inelastic tunneling between the initial and final state, that is, during the transfer of the electron (or hole) vibrational quanta are absorbed and emitted by the electron (or hole). The term after A_{-1} contains the emission of one quantum, and the A_{+1} term contains the absorption of one quantum. The two vibrational quanta inelastic tunneling processes are described by the A_2 terms.

C. Localized States versus Partly Delocalized States Hopping: Which Channel Dominates? In the calculation, we distinguish between two channels of thermally activated hopping, via localized and via partially delocalized states.

Depending on the electronic couplings and reorganization energies of the states, it will be easier for the hole, initially localized at the donor G, to reach a localized or a partly delocalized state in the bridge. The overall efficiency of a channel then depends on the probability to reach a certain state and on the transfer efficiency between the states (localized or delocalized) within one channel. In the limit where the electronic coupling is comparable to or larger than the reorganization energy of a local hole state, the splitting between electronic eigenstates of the bridge will determine the gap between donor and bridge. In addition, electronic delocalization decreases the

nuclear reorganization energy of the states and thus leads to fast intrabridge rates. Those two effects are responsible for a faster transfer through the delocalized states channel.

If, on the other hand, the reorganization energy of localized states is larger than the electronic coupling, the equilibrium constant is shifted in favor of thermal activation of the localized states. This effect can overcompensate the decrease in transfer efficiency between localized states caused by the larger reorganization energy, and the localized states channel will dominate.

An interesting effect is observed in the presence of static disorder. The latter barely changes the transfer efficiency in the first limit of strong electronic coupling, but it strongly decreases the transfer efficiency via localized states hopping. This decrease is a result of local barriers created by the disorder in the bridge. Because the localized states hopping is a nearest-neighbor hopping, such barriers in the bridge will be critical bottlenecks for the overall transfer rate, and thus, the efficiency of the transfer goes down with increasing disorder. In the case of partly delocalized states, the hole (electron) can tunnel through such local barriers in the bridge, a phenomenon that is termed variable-range hopping.[31] It was used recently by Yu and Song[28] to explain the temperature dependence of conductivity measured[32] in λ-phage DNA. Because of this phenomenon, the transfer efficiency between extended states does not depend as critically as the one for the localized states on the disorder. Hence in a situation where the localized states channel dominates the thermally activated transfer, an increase in disorder in bridge energies will change the branching ratio of the two channels in favor of the delocalized states channel.

Finally, we note that the present formulation in terms of two channels is an approximation of the real situation where just one channel exists that contains partly delocalized states but takes into account a dynamic localization of the states by so-called self-trapping. A more exact but more complicated formulation (involving the solution of a nonlinear Schrödinger equation) in terms of solitary electronic states can be found in a series of papers by Fischer and co-workers (ref 55 and references therein).

D. Explanation of the Flat Distance Dependence of the Hole Transfer Rate. The principal finding in that article is that the delocalization provides at least one explanation of the reported flat distance dependence of the relative yield found by Giese et al.[26] When one uses a phenomenological nearest-neighbor hopping model, the ratio of rate constants, k_B/k_{-1} or k_2/k_{-1}, appearing in eq 8 is large. An explanation of this result is obtained within the present framework by interpreting k_B as an *effective* hopping rate constant, the hole transfer involving partly delocalized states in the bridge. Hence, the hole will not hop between neighboring bases but between larger regions. In addition, this "length" of the hole leads typically to a smaller reorganization energy for transfer in the bridge than for transfer from a local donor or acceptor state into the bridge. This difference in reorganization energies in turn also leads to faster intrabridge transfer.

In the comparison between theory and experiment in Figures 4 and 5, for short ($N < 3$) bridges, the superexchange mechanism dominates, so an exponential distance dependence of the yield results, whereas for $N > 3$, the hole transfer involves thermally populated bridge states. This interpretation of the behavior is now well-known.[13,14]

In the calculation of the thermally activated hopping that occurs at bridge lengths $N > 3$, two different channels, via localized states and via delocalized states, have been taken into account. Furthermore, two different sets of ab initio electronic couplings were considered. Using the couplings obtained by Troisi and Orlandi,[45] we obtain the yields in Figure 4, which show a clear preference of the delocalized states hopping channel. The splitting between electronic bridge states brings some of the bridge states to low enough energies so that thermal activation of the hole at the donor G to those states is easier than thermal activation leading to a localized bridge state. The flat distance dependence results from the efficient transfer between the partly delocalized states due to a small reorganization energy as discussed above and because the splitting between the bridge states is larger for longer bridge lengths thus decreasing the energy gap between donor and bridge even further and so promoting thermal activation. The nonmonotonical behavior obtained in the absence of disorder is due to the symmetry of the electronic states in the bridge and is washed out by the disorder. As discussed before, the variable-range hopping mechanism leads to a relative robustness of the overall hopping rate against static disorder.[58]

The second set of electronic couplings obtained by Voityuk et al.[44] leads to a more complicated situation, as shown in Figure 5 for the present static disorder. Both channels, the one with localized and the one involving partly delocalized bridge states, contribute to the observed yield. As before, the delocalized states hopping shows a weaker distance dependence than the localized states hopping. An interesting difference with respect to the calculations in Figure 4 concerns the disorder dependence of the delocalized states hopping. It increases with increasing disorder, as shown in the right part of Figure 5, whereas it did not depend much on distance in the upper part of Figure 4. The difference between the two results is due to the different electronic couplings. In Figure 4, the electronic coupling is strong enough to determine the energy gap between the donor and the bridge. The electronic coupling is an order of magnitude smaller in Figure 5, and in this case, the energy gap between the hole donor G and the bridge is a function of disorder. Disorder in the bridge, which localizes the states, brings some bridge energies closer to the energy of the donor state, as discussed below, and thus thermal activation becomes more likely via these states, and the relative yield increases with disorder. This effect of decreasing the energy gap between G and the bridge of A's by disorder is explained by the dependence of the reorganization energies of the extended states on the disorder, as discussed in detail in Appendix D.

The question may arise: Is there any set of parameters in the nearest-neighbor hopping model that gives agreement with the reported experiment? This question can be answered by returning to the phenomenological hopping model studied in section 2 that yielded agreement for large values of $x = k_B/k_{-1} + k_B/k_2$, where k_B is the hopping rate constant between neighboring bridge sites and k_{-1} (k_2) is the rate constant for transfer between the first (last) bridge site and the donor (acceptor). In Appendix E, several possible reasons for a large x are discussed, but we judge them to be improbable. Recently,[59] we became aware of an alternative explanation in terms of localized states that is based on quantum chemical calculations[60] of hole energies of base pair triplets. It involves local barriers created at the first and last A in the bridge. Such barriers would be due to the different nearest-neighbor bases seen by those terminal A's of the bridge. Applying the triplet rule of Voityuk et al.,[60] a $-\Delta G^\circ = 234$ meV for the hole transfer from the first to the second A in the bridge and a $-\Delta G^\circ = -127$ meV for the transfer between the $(N-1)$th and the Nth A in the bridge are obtained. Because the latter value is smaller than zero, the

corresponding rate can be assumed to be slower than the rates between the other A's in the bridge (which have $-\Delta G^\circ = 0$ or 234 meV). Therefore the hole transfer between the $(N-1)$th and the Nth A in the bridge can create a bottleneck of the reaction on the basis of the quantum chemical calculations.[60] However, we note that this bottleneck effect will be much weaker if variable-range hopping is included in the theory because the hole can tunnel through the terminal A's. To help to settle this question, experiments on a DNA duplex in which G, A_N, and GGG are placed in one 5′-G-$(A)_N$-GGG-3′ strand (instead of having G and A at different strands) would be helpful. In this case, if the triplet rule[60] is correct, there are no bottlenecks at the terminal A's and the localized state hopping model then predicts a steeper distance dependence, whereas the delocalized state hopping model predicts still a flat distance dependence.

E. Discussion of Dynamic and Static Disorder. The disorder is both dynamic, described by the spectral density $J(\omega)$, and static, described by Δ_{dis}. The two forms of disorder have their origin in the conformational dynamics of DNA and the solution.

The fast fluctuation of the DNA structure leads to a dynamic modulation of local hole energies and is treated by the spectral density $J(\omega)$. This $J(\omega)$ was extracted here from fluorescence and absorption line shapes of intercalated ethidium. It is a simplification to assume that the modulation of the optical transition energy is the same as the fluctuation of a local hole energy. However, the extracted $J(\omega)$ results in a reorganization energy $\lambda = 0.48$ eV for hole transfer between two localized states, which is close to the 0.4 eV estimated[6] from time-resolved measurements[5,6] of hole transfer between two intercalated ethidium molecules. Our estimated $\lambda = 0.48$ eV is about half of the reorganization energy obtained in experiments on DNA hairpins.[61] In these hairpins, the hole donor, a stilbene, is exposed to the solvent, which may explain at least part of the larger reorganization energy (see Appendix F). Cho and Fleming[62] investigated how the two types of spectral densities, those for optical transitions and those for electron transfer, are related. They concluded that the same functional form of $J(\omega)$ can be assumed but that the two spectral densities can differ by a scaling factor. We have set this scaling factor to unity on the basis of a comparison of the reorganization energy obtained with experimental values. (The scaling factor can be expected to depend on the tightness of the pair in the excitation.)

Any dynamics that is slow compared to the charge-transfer process is considered as static disorder and described by a distribution in site energies.[63] Here, a Gaussian distribution of width (fwhm) $\Delta_{dis} = 0.08$ eV was estimated. This value is smaller, and is expected to be smaller, than the value of 0.15 eV used by Yu and Song[28] to explain the temperature dependence of conduction measured[32] in λ-DNA because in the latter study an additional change of local energies by a random DNA sequence had to be considered.

VI. Summary

We summarize the results obtained in the present paper as follows: An electron (hole) transfer rate constant for vibrationally induced transitions between extended electronic states was derived. The rate constant includes the tunneling, as well as the hopping-like, transfer of the electron (hole). An explanation of the reported flat distance dependence of the relative yield of strand cleavage measured by Giese et al. for long bridges ($N > 3$) is given. It involves thermally activated transfer between *partly delocalized* states of the bridge and disorder. An interesting effect of disorder found here is that it suppresses the thermally activated hopping via localized states and promotes the hopping via partly delocalized states because of variable-range hopping and the disorder dependence of reorganization energies of the extended states.

Acknowledgment. One of us (T.R.) acknowledges support of a Lynen Research Fellowship from the Alexander von Humboldt Foundation and support by the Deutsche Forschungsgemeinschaft (Emmy Noether Grant RE 1610/1-1). Support by the National Science Foundation and the Office of Naval Research is also acknowledged. We thank C. Treadway and T. Fiebig for providing us the absorption and fluorescence spectra, and we thank S. Gosavi for stimulating discussions. It is a pleasure to acknowledge valuable discussions with A. Okada, S. Tanaka, and H. Sumi. Further discussions with M. E. Michel-Beyerle and S. F. Fischer and a comment by J. Jortner were also very helpful.

Appendix A: Derivation of the Effective Hopping Rate Constant, $k_h^{eff}(N)$

In steady-state approximation for the A_n's, eq 1b can be written as

$$A_1 = \frac{-k_1 G}{-(k_B + k_{-1}) + k_B \dfrac{A_2}{A_1}} \tag{A1}$$

and for $j = 2$ to $N-1$, the following recursion relation is obtained from eq 1c

$$\frac{A_j}{A_{j-1}} = \frac{1}{2 - \dfrac{A_{j+2}}{A_{j+1}}} \tag{A2}$$

From eq 1d, we have

$$\frac{A_N}{A_{N-1}} = \left(1 + \frac{k_2}{k_B}\right) \Big/ \left(1 - \frac{k_{-2}}{k_B + k_2}\frac{GGG}{A_N}\right) \tag{A3}$$

Equation A2 defines a continued fraction that is terminated by the A_N/A_{N-1} in eq 73. From these two equations, an explicit formula for $A_{N-n}/A_{N-(n+1)}$ is obtained

$$\frac{A_{N-n}}{A_{N-(n+1)}} = \frac{n - (n-1)A_N/A_{N-1}}{n + 1 - nA_N/A_{N-1}} \qquad n = 0 \text{ to } N-2 \tag{A4}$$

The preceding equation and eq A3 are then used to obtain

$$\frac{A_n}{A_N} = \frac{k_2}{k_B}(N-n) + 1 - (N-n)\frac{k_{-2}}{k_B}\frac{GGG}{A_N} \tag{A5}$$

Introduction of eq A5 for $n = 2$ into eq A1 yields a relation between A_1 and A_N, while eq A5 for $n = 1$ yields a second relation. Elimination of A_1 yields

$$A_N = \frac{\dfrac{k_1}{k_{-1}}\dfrac{k_B}{k_2}}{N - 1 + \dfrac{k_B}{k_{-1}} + \dfrac{k_B}{k_2}} G + \frac{\dfrac{k_{-2}}{k_2}\left(N - 1 + \dfrac{k_B}{k_{-1}}\right)}{N - 1 + \dfrac{k_B}{k_{-1}} + \dfrac{k_B}{k_2}} GGG \tag{A6}$$

From eqs A6 and A5 for $n = 1$, A_1 is obtained as

$$A_1 = \frac{\frac{k_1}{k_{-1}}\left(N-1+\frac{k_B}{k_2}\right)}{N-1+\frac{k_B}{k_{-1}}+\frac{k_B}{k_2}}G + \frac{\frac{k_{-2}}{k_2}\frac{k_B}{k_{-1}}}{N-1+\frac{k_B}{k_{-1}}+\frac{k_B}{k_2}}GGG \quad (A7)$$

By introducing eq A7 into eq 1a and eq A6 into eq 1e, the equations 2a and 2b of the text are obtained with the effective rate constants given in eqs 3 and 4.

Appendix B: Derivation of an Expression for the Rate Constant $k_{M\to N}$

The Liouville-von Neumann equation for the statistical operator reads[64]

$$\frac{d}{dt}\hat{W}_{MN} = -i\omega_{MN}\hat{W}_{MN} + \frac{1}{i\hbar}(H_{vib}(M)\hat{W}_{MN} - \hat{W}_{MN}H_{vib}(N)) + \frac{1}{i\hbar}\sum_L(\hat{V}_{ML}\hat{W}_{LN} - \hat{W}_{ML}\hat{V}_{LN}) \quad (B1)$$

where the coupling $\hat{V}_{MN}$, the energy difference $\hbar\omega_{MN}$, and vibrational Hamiltonian of the Mth PES $H_{vib}(M)$ were defined in the text in eqs 20, 23, and 26, respectively.

For a perturbation treatment of the coupling $\hat{V}_{MN}$, the following interaction representation of the statistical operator is used

$$\hat{W}^{(I)}_{MN}(t) = e^{i\omega_{MN}t}\,U^\dagger_M(t)\hat{W}_{MN}(t)U_N(t) \quad (B2)$$

where the time-evolution operator $U_M(t)$ is given in eq 25. The equation of motion for the statistical operator in eq B2 is

$$\frac{d}{dt}\hat{W}^{(I)}_{MN}(t) = \frac{1}{i\hbar}\sum_L(\hat{V}^{(I)}_{ML}(t)\hat{W}^{(I)}_{LN}(t) - \hat{W}^{(I)}_{ML}(t)\hat{V}^{(I)}_{LN}(t)) \quad (B3)$$

with

$$\hat{V}^{(I)}_{MN}(t) = e^{i\omega_{MN}t}\,U^\dagger_M(t)\hat{V}_{MN}U_N(t) \quad (B4)$$

Equation B3 leads to a second-order generalized rate equation for the population $P_M(t)$,

$$P_M(t) = tr_{vib}\{\hat{W}_{MM}(t)\} = tr_{vib}\{\hat{W}^{(I)}_{MM}(t)\} \quad (B5)$$

namely

$$\frac{d}{dt}P_M(t) = -Re\sum_N\int_0^t d\tau\,[k_{M\to N}(\tau)P_M(t-\tau) - k_{N\to M}(\tau)P_N(t-\tau)] \quad (B6)$$

with a generalized rate constant

$$k_{M\to N}(t) = e^{i\omega_{MN}t}\frac{2}{\hbar^2}\,tr_{vib}\{U^\dagger_M(t)\hat{V}_{MN}U_N(t)\hat{V}_{NM}W_{eq}(M)\} \quad (B7)$$

When $k_{M\to N}(t)$ decays rapidly on the time scale of the dissipative dynamics of the occupation probabilities, $P_M(t)$ and $P_N(t)$ of eq B6, then the occupation probabilities can be extracted from the integral by approximating them by their value at time t, that is, $P_M(t-\tau) \approx P_M(t)$. The upper integration limit in eq B6 may then be replaced by $+\infty$, and one obtains the rate equation 21 of the text with the rate constant eq 22 obtained from

$$k_{M\to N} = \frac{1}{2}\int_{-\infty}^{\infty} dt\, k_{M\to N}(t) \quad (B8)$$

where the property $k_{M\to N}(t) = k^*_{M\to N}(-t)$ of the generalized rate eq B7 was used.

To calculate the generalized rate in eq B7, the trace has to be performed over the thermally equilibrated vibrational states of the Mth PES. The PES's of states $|M\rangle$ and $|N\rangle$ are shifted parabolas. This shift can formally be expressed by a shift operator:[65]

$$D^\dagger_M = \exp\sum_\xi\{g_\xi(M,M)(C_\xi - C^\dagger_\xi)\} \quad (B9)$$

Any operator O_M that depends on the coordinates of the shifted PES M is changed using $O_M = D^\dagger_M O_0 D_M$. In particular, the time-evolution operator for the unshifted PES,

$$U_0 = \exp\left\{-\frac{it}{\hbar}\sum_\xi\frac{\hbar\omega_\xi}{4}(Q_\xi{}^2 + P_\xi{}^2)\right\}$$

becomes

$$U_M(t) = \exp\{-(i/\hbar)t\sum_\xi(\hbar\omega_\xi/4)((Q_\xi + 2g_\xi(M,M))^2 + P^2_\xi)\} \quad (B10)$$

Similarly, eq B7 can be written as

$$k_{M\to N}(t) = e^{i\omega_{MN}t}\frac{2}{\hbar^2}\,tr_{vib}\{D^\dagger_M U^\dagger_0(t)D_M\hat{V}_{MN}D^\dagger_N U_0(t)D_N\hat{V}_{NM}D^\dagger_M W^{(0)}_{eq}D_M\} = e^{i\omega_{MN}t}\frac{2}{\hbar^2}\,tr_{vib}\{U^\dagger_0(t)D_M\hat{V}_{MN}D^\dagger_M D_M D^\dagger_N U_0(t)D_N D^\dagger_M D_M\hat{V}_{NM}D^\dagger_M W^{(0)}_{eq}\} \quad (B11)$$

With the use of the identity

$$D_M(C_\xi + C^\dagger_\xi)D^\dagger_M = C_\xi + C^\dagger_\xi - 2g_\xi(M,M) \quad (B12)$$

and of the definition of the couplings $\hat{V}_{MN}$ (eq 20), the $D_M\hat{V}_{MN}D^\dagger_M$ in eq B11 then is

$$D_M\hat{V}_{MN}D^\dagger_M = \hat{V}_{MN} - 2K_r \quad (B13)$$

where a reorganization energy

$$K_r = K_r(M,N) = \sum_\xi\hbar\omega_\xi g_\xi(M,N)g_\xi(M,M) \quad (B14)$$

was introduced. The $k_{M\to N}(t)$ in eq B11 becomes

$$k_{M\to N}(t) = e^{i\omega_{MN}t}\frac{8K_r^2}{\hbar^2}\,tr_{vib}\left\{U^\dagger_0(t)\left(1-\frac{\hat{V}_{MN}}{2K_r}\right)\times U_0(t)U^\dagger_0(t)D_{MN}U_0(t)D^\dagger_{MN}\left(1-\frac{\hat{V}_{MN}}{2K_r}\right)W^{(0)}_{eq}\right\} \quad (B15)$$

where a new shift operator, D_{MN}, was introduced

$$D_{MN} = D_M D^\dagger_N = \exp\{-\sum_\xi\Delta g_\xi(C_\xi - C^\dagger_\xi)\} \quad (B16)$$

Here $\Delta g_\xi = \Delta g_\xi(M,N) = g_\xi(M,M) - g_\xi(N,N)$. In evaluating eq B15, it is convenient[66] to introduce two exponentials, $\exp(-\lambda_1(\hat{V}_{MN}/(2K_r)))$ and $\exp(-\lambda_2(\hat{V}_{MN}/(2K_r)))$, and to define a function, $f(\lambda_1,\lambda_2)$, as

$$f(\lambda_1,\lambda_2) = e^{i\omega_{MN}t}\frac{8K_r^2}{\hbar^2}\,\mathrm{tr}_{vib}\left\{\exp\left(-\lambda_1\frac{\hat{V}_{MN}(t)}{2K_r}\right)D_{MN}(t)D_{MN}^{\dagger}\exp\left(-\lambda_2\frac{\hat{V}_{MN}}{2K_r}\right)W_{eq}^{(0)}\right\} \quad \text{(B17)}$$

an expansion of which retaining only the first two terms and setting $\lambda_1 = \lambda_2 = 1$ yields eq B15. The use of such a function will make it possible to apply a second-order cumulant expansion for the evaluation of expectation values as shown below.

The time-dependence of $\hat{V}_{MN}(t)$ and $D_{MN}(t)$ is given by the time-evolution operator, $U_0(t)$, as that

$$\exp\left(-\lambda_1\frac{\hat{V}_{MN}(t)}{2K_r}\right) = U_0^{\dagger}(t)\exp\left(-\lambda_1\frac{\hat{V}_{MN}}{2K_r}\right)U_0(t) = \exp(-\lambda_1\sum_{\xi}v_{\xi}(C_{\xi}e^{-i\omega_{\xi}t} + C_{\xi}^{\dagger}e^{i\omega_{\xi}t})) \quad \text{(B18)}$$

$$D_{MN}(t) = U_0^{\dagger}(t)D_{MN}U_0(t) = \exp(-\sum_{\xi}\Delta g_{\xi}(C_{\xi}e^{-i\omega_{\xi}t} - C_{\xi}^{\dagger}e^{i\omega_{\xi}t})) \quad \text{(B19)}$$

where a scaled coupling constant v_ξ was introduced:

$$v_{\xi} = v_{\xi}(M,N) = \hbar\omega_{\xi}g_{\xi}(M,N)/(2K_r) \quad \text{(B20)}$$

Using the relation $e^A e^B = e^{A+B}e^{1/2[A,B]}$, valid when the higher-order commutators, such as $[A,[A,B]]$, vanish, one obtains for $A = \sum_\xi(a_{1\xi}C_\xi + a_{2\xi}C_\xi^{\dagger})$ and $B = \sum_\xi(a_{3\xi}C_\xi + a_{4\xi}C_\xi^{\dagger})$

$$e^A e^B = \exp\left(\sum_{\xi}((a_{1\xi}+a_{3\xi})C_{\xi} + (a_{2\xi}+a_{4\xi})C_{\xi}^{\dagger})\right)\exp\left(\frac{1}{2}\sum_{\xi}(a_{1\xi}a_{4\xi} - a_{2\xi}a_{3\xi})\right) \quad \text{(B21)}$$

The first product in eq B17 using the above relation becomes

$$\exp\left(-\lambda_1\frac{\hat{V}_{MN}(t)}{2K_r}\right)D_{MN}(t) = \exp\left(\sum_{\xi}\{-(\lambda_1 v_{\xi} + \Delta g_{\xi})e^{-i\omega_{\xi}t}C_{\xi} + (\Delta g_{\xi} - \lambda_1 v_{\xi})e^{i\omega_{\xi}t}C_{\xi}^{\dagger}\}\right)\exp\left(-\sum_{\xi}\lambda_1 v_{\xi}\Delta g_{\xi}\right) \quad \text{(B22)}$$

Treating the remaining products in the same way yields

$$f(\lambda_1,\lambda_2) = \frac{8K_r^2}{\hbar^2}e^{i\omega_{MN}t}\exp\left(-(\lambda_1+\lambda_2)\sum_{\xi}\Delta g_{\xi}v_{\xi}\right)\exp\left(\frac{1}{2}\sum_{\xi}\{(\Delta g_{\xi}+\lambda_2 v_{\xi})(\Delta g_{\xi}+\lambda_1 v_{\xi})e^{-i\omega_{\xi}t} - (\Delta g_{\xi} - \lambda_2 v_{\xi})(\Delta g_{\xi} - \lambda_1 v_{\xi})e^{i\omega_{\xi}t}\}\right)\mathrm{tr}_{vib}\{\exp\left(\sum_{\xi}(a_{1\xi}C_{\xi} + a_{2\xi}C_{\xi}^{\dagger})\right)W_{eq}^{(0)}\} \quad \text{(B23)}$$

The coefficients in the last line read $a_{1\xi} = \Delta g_\xi - \lambda_2 v_\xi - (\Delta g_\xi + \lambda_1 v_\xi)e^{-i\omega_\xi t}$ and $a_{2\xi} = -(\Delta g_\xi + \lambda_2 v_\xi) + (\Delta g_\xi - \lambda_1 v_\xi)e^{i\omega_\xi t}$, where a second-order cumulant expansion, which is exact for harmonic oscillators, gives for the thermal average in eq B23

$$\mathrm{tr}_{vib}\left\{\exp\left(\sum_{\xi}(a_{1\xi}C_{\xi} + a_{2\xi}C_{\xi}^{\dagger})\right)W_{eq}^{(0)}\right\} = \exp\left(\frac{1}{2}\sum_{\xi}a_{1\xi}a_{2\xi}(1+2n(\omega_{\xi}))\right) \quad \text{(B24)}$$

where

$$n(\omega_{\xi}) = \mathrm{tr}_{vib}\{C_{\xi}^{\dagger}C_{\xi}W_{eq}^{(0)}\} = \frac{1}{e^{\hbar\omega_{\xi}/(kT)} - 1} \quad \text{(B25)}$$

was introduced. The function $f(\lambda_1,\lambda_2)$ then follows as

$$f(\lambda_1,\lambda_2) = e^{-i\omega_{MN}t}\frac{8K_r^2}{\hbar^2}e^{\phi_{MN}(t)-\phi_{MN}(0)}e^{(\lambda_1+\lambda_2)(\tilde{G}_{MN}(t)-\tilde{G}_{MN}(0))}e^{\lambda_1\lambda_2\tilde{F}_{MN}(t)}e^{(\lambda_1^2+\lambda_2^2)\tilde{F}_{MN}(0)} \quad \text{(B26)}$$

where $\phi_{MN}(t)$, $\tilde{G}_{MN}(t)$, and $\tilde{F}_{MN}(t)$ denote the functions

$$\phi_{MN}(t) = \sum_{\xi}\Delta g_{\xi}^2((1+n(\omega_{\xi}))e^{-i\omega_{\xi}t} + n(\omega_{\xi})e^{i\omega_{\xi}t}) \quad \text{(B27)}$$

$$\tilde{G}_{MN}(t) = \sum_{\xi}\Delta g_{\xi}v_{\xi}((1+n(\omega_{\xi}))e^{-i\omega_{\xi}t} - n(\omega_{\xi})e^{i\omega_{\xi}t}) \quad \text{(B28)}$$

and

$$\tilde{F}_{MN}(t) = \sum_{\xi}v_{\xi}^2((1+n(\omega_{\xi}))e^{-i\omega_{\xi}t} + n(\omega_{\xi})e^{i\omega_{\xi}t}) \quad \text{(B29)}$$

v_ξ being defined in eq B20. Finally, expanding eq B26 up to bilinear terms in λ_1 and λ_2 and setting $\lambda_1 = \lambda_2 = 1$ yields

$$k_{M\to N}(t) = 2e^{i\omega_{MN}t}e^{\phi_{MN}(t)-\phi_{MN}(0)}\left[\left(\frac{2K_r}{\hbar} + G_{MN}(t) - G_{MN}(0)\right)^2 + F_{MN}(t)\right] \quad \text{(B30)}$$

where $G_{MN}(t) = (2K_r/\hbar)\tilde{G}_{MN}(t)$ and $F_{MN}(t) = (4K_r^2/\hbar^2)\tilde{F}_{MN}(t)$. The time-dependent functions entering the generalized rate constant can be expressed in terms of spectral densities

$$J_{MN,KL}(\omega) = \sum_{\xi}g_{\xi}(M,N)g_{\xi}(K,L)\delta(\omega - \omega_{\xi}) \quad \text{(B31)}$$

The function $\phi_{MN}(t)$ is related to the spectral density containing the shift $\Delta g_\xi^2 = g_\xi(M,M)^2 + g_\xi(N,N)^2 - 2g_\xi(M,M)g_\xi(N,N)$

$$\phi_{MN}(t) = \int_{-\infty}^{+\infty}d\omega\, e^{-i\omega t}(1+n(\omega))([J_{MM,MM}(\omega) + J_{NN,NN}(\omega) - 2J_{MM,NN}(\omega)] - [J_{MM,MM}(-\omega) + J_{NN,NN}(-\omega) - 2J_{MM,NN}(-\omega)]) \quad \text{(B32)}$$

where $J_{MN,KL} = 0$ for $\omega < 0$ and also the relation $n(\omega) = -(1 + n(-\omega))$ were used. The notation in terms of $J_{MN,KL}(-\omega)$ in eq B32 and below does allow one to relate different time-dependent functions to a single function $\phi_n(t)$ in eq 32 in the text.

The function $F_{MN}(t)$ contains the off-diagonal parts, $g_\xi(M,N)$, of the coupling

$$F_{MN}(t) = \int_{-\infty}^{+\infty}d\omega\, e^{-i\omega t}(1+n(\omega))\omega^2[J_{MN,MN}(\omega) - J_{MN,MN}(-\omega)] \quad \text{(B33)}$$

And the function $G_{MN}(t)$ contains the mixed contributions

$$G_{MN}(t) = \int_{-\infty}^{+\infty} d\omega\, e^{-i\omega t}(1 + n(\omega))\omega[J_{MM,MN}(\omega) - J_{NN,MN}(\omega) - J_{MM,MN}(-\omega) + J_{NN,MN}(-\omega)] \quad \text{(B34)}$$

The quantity $2(K_r/\hbar) - G_{MN}(0)$ in eq B30 can be obtained from the above spectral density via

$$2\frac{K_r}{\hbar} - G_{MN}(0) = \frac{\lambda_{MN}}{\hbar} = \int_0^{\infty} d\omega\, \omega(J_{MMMN}(\omega) + J_{NNMN}(\omega)) \quad \text{(B35)}$$

where a new reorganization energy λ_{MN} was introduced. The generalized rate constant becomes

$$k_{M\to N}(t) = 2e^{i\omega_{MN}t}\, e^{\phi_{MN}(t)-\phi_{MN}(0)}\left[\left(\frac{\lambda_{MN}}{\hbar} + G_{MN}(t)\right)^2 + F_{MN}(t)\right] \quad \text{(B36)}$$

Neglecting in eq 15 the dynamic modulation of the electronic couplings, that is, setting $\Delta V_{ij}(\xi) = 0$ and assuming that the electronic energies at different sites fluctuate independently, the spectral density eq B31 becomes

$$J_{MN,KL}(\omega) = \sum_i c_i^{(M)} c_i^{(N)} c_i^{(K)} c_i^{(L)} \sum_\xi \left(\frac{\Delta E_i(\xi)}{\hbar\omega_\xi}\right)^2 \delta(\omega - \omega_\xi) \quad \text{(B37)}$$

If the local coupling constants $\Delta E_i(\xi)$ are assumed to be independent of the site index i, that is, there is the same local modulation of the site energy, eq B37 becomes

$$J_{MN,KL}(\omega) = J(\omega)\sum_i c_i^{(M)} c_i^{(N)} c_i^{(K)} c_i^{(L)} \quad \text{(B38)}$$

in terms of the local spectral density in eq 34. The reorganization energy λ_{MN} in eq 35 then is obtained from eq B35 using eq B38. The time-dependent functions eqs B27, B28, and B29 can then be expressed in terms of a function $\phi_n(t)$ in eq 32 as shown in eqs 29−31. Using eqs 29−31, together with eq B36 and B8, one arrives at the $k_{M\to N}$ in eq 28.

Appendix C: Relation of the Rate $k_{M\to N}$ to an Expression Derived Earlier by Okada, Zhang, Meier, Chernyak, and Mukamel

Using the Brownian oscillator approach[29] and a projection operator technique, Mukamel and co-workers[14,53,54] derived a rate constant that is identical with the present result in the limit of a large number of primary oscillators and zero damping by the bath oscillators, as will be shown in the following. The function $g(t)$ of the Brownian oscillator approach in this limit and the functions $\phi_n(t)$ in eq 32 and reorganization energy E_λ in eq 36 in the present treatment are related by[29]

$$g(t) = \phi_0(0) - \phi_0(t) - it\frac{E_\lambda}{\hbar} \quad \text{(C1)}$$

For the calculation of the rate constant in ref 53, the first and second derivatives of $g(t)$ are needed. They are

$$\dot g = -\dot\phi_0(t) - i\frac{E_\lambda}{\hbar} = i\left(\phi_1(t) - \frac{E_\lambda}{\hbar}\right) \quad \text{(C2)}$$

and

$$\ddot g = \phi_2(t) \quad \text{(C3)}$$

The rate constant $k_{M\to N}$, given in eqs A24, C6, and C17−C19 of ref 53, reads

$$k_{M\to N} = \int_{-\infty}^{\infty} dt\, K_{NM}^{L}(t) \quad \text{(C4)}$$

with

$$K_{NM}^{L}(t) = K_{NM}^{F}(t)\{\ddot g_{NM,MN}(\tau) - [\dot g_{MN,MM}(\tau) - \dot g_{MN,NN}(\tau) + 2i\lambda_{MN,MM}][\dot g_{MM,NM}(\tau) - \dot g_{NN,NM}(\tau) + 2i\lambda_{NM,MM}]\} \quad \text{(C5)}$$

where $K_{NM}^{F}(t)$ is

$$K_{NM}^{F}(t) = \exp\left\{-\frac{i}{\hbar}(\mathcal{O}_N - \mathcal{O}_M)t - g_{NN,NN}(t) - g_{MM,MM}(t) + g_{MM,NN}(t) + g_{NN,MM}(t) - 2i(\lambda_{MM,MM} - \lambda_{NN,MM})t\right\} \quad \text{(C6)}$$

and the λ's are defined as

$$\lambda_{MNKL} = -\lim_{t\to\infty} \mathrm{Im}[\dot g_{MNKL}(t)] \quad \text{(C7)}$$

For localized vibrations considered there,[53] as well as in the present paper, the function $g_{MNKL}(t)$ is

$$g_{MNKL}(t) = \sum_n c_n^{(M)} c_n^{(N)} c_n^{(K)} c_n^{(L)} g(t) \quad \text{(C8)}$$

and therefore it holds also $\dot g_{MNKL}(t) = \sum_n c_n^{(M)} c_n^{(N)} c_n^{(K)} c_n^{(L)} \dot g(t)$. The function λ_{MNKL} in eq C7 then follows, using eq C2, as

$$\lambda_{MNKL} = \sum_n c_n^{(M)} c_n^{(N)} c_n^{(K)} c_n^{(L)} E_\lambda \quad \text{(C9)}$$

With the use of eqs C1, C8, and C9, the function $K_{NM}^{F}(t)$ in eq C6 becomes

$$K_{NM}^{F}(t) = e^{i\omega_{MN}t + \phi_{MN}(t) - \phi_{MN}(0)} \quad \text{(C10)}$$

where the function $\phi_{MN}(t)$ is given in eq 29 and the ω_{MN} is defined in eqs 23 and 17. The fact that the λ_M in eq 17 equals λ_{MMMM} was used.

From eqs C3 and C8, the $\ddot g_{NM,MN}(\tau)$ in eq C5 is seen to equal the function $F_{MN}(\tau)$ in eq 31,

$$\ddot g_{NM,MN}(\tau) = F_{MN}(\tau) \quad \text{(C11)}$$

The product of square brackets on the rhs of eq C5 can be written in terms of the functions $G_{MN}(t)$ in eq 30 and λ_{MN} in eq 35,

$$[\ddot g_{MN,MM}(\tau) - \dot g_{MN,NN}(\tau) + 2i\lambda_{MN,MM}][\dot g_{MM,NM}(\tau) - \dot g_{NN,NM}(\tau) + 2i\lambda_{NM,MM}] = \left(\frac{\lambda_{MN}}{\hbar} + G_{MN}(\tau)\right)^2 \quad \text{(C12)}$$

where eqs C2, C8, and C9 were used. Equation 28 of the text is obtained by introducing eqs C10−C12 into eqs C5 and C4.

Appendix D: Disorder Dependence of Thermal Activation for Weak Electronic Couplings

The more delocalized the states of the bridge are, the smaller is their solvation-vibrational reorganization energy λ_M in eq 37. Any ion reorganization energy accompanying the hole transfer might be included in a reorganization energy as one possibility

(ref 67 and references therein). Because the states at G and GGG are strongly localized, their energies are shifted by E_λ, whereas the bridge energies are shifted by less than E_λ because $L_M > 1$ for these states. The size of L_M depends on the relative strength of electronic coupling and disorder. The energy difference $\hbar\omega_{GM}$, eq 23, that enters the rate constant $k_{G\rightarrow M}$ for thermal activation from a state localized at G to a bridge state M then is (eq 62)

$$\hbar\omega_{GM} = (\mathcal{E}_G - \lambda) - \left(\mathcal{E}_M - \frac{\lambda}{L_M}\right) \qquad \text{(D1)}$$

where $\mathcal{E}_G$ and $\mathcal{E}_M$ are the eigenenergies obtained from the site energies and couplings by a diagonalization procedure at the equilibrium configuration of the ground state (no charge carrier present). Because the state G is strongly localized at G, L_G was set to unity as discussed above. Because L_M will always decrease with increasing disorder, on average, the absolute value of the energy difference $\hbar\omega_{GM}$ will become smaller, and therefore, thermal activation from G to M will become more likely.

Appendix E: Possible Alternative Explanations of the Flat Distance Dependence within the Nearest-Neighbor Hopping Model

Within a nearest-neighbor hopping model, the large value of x from eq 8 is unexpected because the free energy difference, $-\Delta G°$, for hole transfer from the bridge to either the G or the GGG is larger than that for transfer inside the bridge. A possible explanation for such large x then could be that the hopping from the bridge to the GGG and (or) to the G happens in the inverted regime of electron transfer. To decide whether the individual transfer steps occur in the normal or in the inverted region of electron transfer, the standard free energy, $\Delta G°$, of an individual reaction step has to be compared with the reorganization energy, λ, for that step. There are no direct measurements of $\Delta G°$ and λ for all of the individual steps. A detailed discussion of estimates resulting from different experimental[47,48,57,61] and theoretical[60,68] studies is given in Appendix F. Those estimates provide no indication for the presence of a $-\Delta G°$ that is larger than the reorganization energy.

Another possible explanation for the large x could be that the reorganization energies for the hopping from the bridge are much larger than those for the intrabridge hopping. In a numerical study on a model donor−bridge−acceptor system,[16] the peculiar case in which the two reorganization energies differ by an order of magnitude lead to a flat distance dependence. Because in the present system neither the G nor the GGG are solvent-exposed, such a difference in reorganization energies is not easy to understand. However, as we saw before in an extended states model, the extension of the bridge states decreases their reorganization energies and thus gives faster transfer.

Another possibility is a difference in electronic couplings for inter- and intrastrand transfer,[69] because the transfer in the bridge is of the former and the transfer from G to A and from A to GGG is of the latter type. Recent ab initio calculations[44,45] yielded different results. In ref 44, similar intrastrand A−A and interstrand G−A couplings were obtained, whereas in ref 45, the interstrand G−A couplings were calculated to be 1 order of magnitude smaller than the intrastrand A−A couplings. Nevertheless, as seen in Figure 4, the localized states model predicts a steeper distance dependence than is observed in the experiment also for the latter difference in interstrand and intrastrand couplings.

In summary, the microscopic parameters that would explain the flatness of the experimental curve within a nearest-neighbor hopping model seem unlikely in the light of recent independent experiments and theoretical calculations.

Appendix F: Estimate of Free Energies and Reorganization Energies

For a hole transfer from G to A, that is, for the reaction $G^+ + A \rightarrow G + A^+$, $-\Delta G°$ in the gas phase can be estimated from the vertical ionization potentials for G and A in the gas phase to be approximately 0.2 eV.[47] From measurements of oxidation potentials in acetonitrite solution,[48] a value of 0.47 eV is inferred for $-\Delta G°$. However, $\Delta G°$ may well be solvent-dependent. Recently, the effect of neighboring bases on the value of the local hole energies has been estimated theoretically.[60] It was inferred that, except for bases close to the terminal, the nearest neighbors of a base have the strongest influence on the energy of a local hole at that base. If correct, the free energy difference for hole transfer between two bases X and Y, where X has nearest neighbors S and V and Y has nearest neighbors W and Z can be estimated from the difference of local hole energies of the triplets SX^+V and WY^+Z. The local hole energies were calculated for all possible combination of triplet bases in ref 60. On this highly uncertain basis, $-\Delta G° = 0.36$ eV would be deduced for the reaction $A^+ + G \rightarrow A + G^+$ at the GGG side of the bridge.

Different values for λ have been measured in different systems: $\lambda = 0.4$ eV was measured for hole transfer between intercalated ethidium molecules,[5,6] and $\lambda = 1.22$ eV was reported from time-resolved measurements of hole transfer between a solvent-exposed stilbene and a neighboring guanine in DNA hairpins.[61] The latter λ was decomposed into a contribution $\lambda_s = 0.23$ eV from low-frequency solvent modes and a contribution $\lambda_i = 0.99$ eV from a high-frequency (1500 cm^{-1}) quantum mode.[61] However, the distinction between intermolecular and intramolecular contributions to λ on the basis of a measured rate constant is quite uncertain, and hence, the influence of the solvent could have been different than assumed there.[61] Recent quantum chemical and molecular dynamics calculations of Tanaka and Sengoku[68] on the same hairpin yielded a somewhat larger $\lambda = 1.51$ eV and a contribution of 1.25 eV to that λ from low-frequency modes with energies smaller than 800 cm^{-1}. Because of the solvent exposure of the stilbene, the λ might have been larger than that in the ethidium study. In a recent experimental study[57] of hole transfer in DNA between an acridine dye and a guanine, $\lambda = 0.6$ eV was determined for a nearest-neighbor reactant pair. For longer distances between hole donor and acceptor, an even larger reorganization energy was reported.[57] All λ's are larger or only slightly smaller than all of the $-\Delta G°$'s.

References and Notes

(1) Murphy, C. J.; Arkins, M. R.; Jenkins, Y.; Ghattia, N. D.; Bossmann, S. H.; Turro, N. J., Barton, J. K. *Science* **1993**, *262*, 1025.
(2) Kelley, S. O.; Barton, J. K. *Science* **1999**, *283*, 375.
(3) Ly, D.; Sanii, L.; Schuster, G. B. *J. Am. Chem. Soc.* **1999**, *121*, 9400.
(4) Henderson, P. T.; Jones, D.; Hampikian, G.; Kan, Y.; Schuster, G. B. *Proc. Natl. Acad. Sci. U.S.A.* **1999**, *96*, 8353.
(5) Brun, A. M.; Harriman, A. *J. Am. Chem. Soc.* **1992**, *114*, 3656.
(6) Harriman, A. *Angew. Chem., Int. Ed.* **1999**, *38*, 945.
(7) Lewis, F. D.; Wu, T.; Zhang, Y.; Letsinger, R. L.; Greenfield, S. R.; Wasielewski, M. R. *Science* **1997**, *277*, 673.
(8) Lewis, F. D.; Wu, T.; Liu, X.; Letsinger, R. L.; Greenfield, S. R.; Miller, S. E.; Wasielewski, M. R. *J. Am. Chem. Soc.* **2000**, *122*, 2889.
(9) Meggers, E.; Michel-Beyerle, M. E.; Giese, B. *J. Am. Chem. Soc.* **1998**, *120*, 12950.
(10) Wan, C.; Fiebig, T.; Schiemann, O.; Barton, J. K.; Zewail, A. H. *Proc. Natl. Acad. Sci. U.S.A.* **2000**, *97*, 14052.
(11) Fukui, K.; Tanaka, K. *Angew. Chem., Int. Ed.* **1998**, *37*, 158.

(12) Gray, H. B.; Winkler, J. R. *Annu. Rev. Biochem.* **1996**, *65* 537.
(13) Felts, A. K.; Pollard, W. T.; Friesner, R. A. *J. Phys. Chem.* **1995**, *99*, 2929.
(14) Okada, A.; Chernyak, V.; Mukamel, S. *J. Phys. Chem. A* **1998**, *102*, 1241.
(15) Petrov, E. G.; May, V. *J. Phys. Chem. A* **2001**, *105*, 10176.
(16) Petrov, E. G.; Shevchenko, Ye. V.; Teslenko, V. I.; May, V. *J. Chem. Phys.* **2001**, *115*, 7107.
(17) Okada, A.; Yokojima, S.; Kurita, N.; Sengoku, Y.; Tanaka, S. *J. Mol. Struct. (THEOCHEM)* **2003**, *630*, 283.
(18) Bixon, M.; Giese, B.; Wessely, S.; Langenbacher, T.; Michel-Beyerle, M. E.; Jortner, J. *Proc. Natl. Acad. Sci. U.S.A.* **1999**, *96*, 11713.
(19) Berlin, Y. A.; Burin, A. L.; Ratner, M. A. *J. Phys. Chem. A* **2000**, *104*, 443.
(20) Berlin, Y. A.; Burin, A. L.; Ratner, M. A. *J. Am. Chem. Soc.* **2001**, *123*, 260.
(21) Bixon, M.; Jortner, J. *J. Phys. Chem. A* **2001**, *105*, 10322.
(22) Wan, C.; Fiebig, T.; Kelley, S. O.; Treadway, C. R.; Barton, J. K.; Zewail, A. H. *Proc. Natl. Acad. Sci. U.S.A.* **1999** *96*, 6014.
(23) Kelley, S. O.; Barton, J. K. *Chem. Biol.* **1998**, *5*, 413.
(24) Bixon, M.; Jortner, J. *J. Am. Chem. Soc.* **2001**, *123*, 12556.
(25) Nakatani, K.; Dohno, C.; Saito, I. *J. Am. Chem. Soc.* **2000**, *122*, 5893.
(26) Giese, B.; Amaudrut, J.; Köhler, A.-K.; Spormann, M.; Wessely, S. *Nature* **2001**, *412*, 318.
(27) Berlin, Y. A.; Burin, A. L.; Ratner, M. A. *Chem. Phys.* **2002**, *275*, 61.
(28) Yu, Z. G.; Song, X. *Phys. Rev. Lett* **2001**, *86*, 6018.
(29) Mukamel, S. *Principles of Nonlinear Optical Spectroscopy*; Oxford University Press: New York, 1995; pp 219, 226.
(30) Georgievskii, Y.; Hsu, C.-P.; Marcus, R. A. *J. Chem. Phys.* **1999**, *110*, 5307.
(31) Mott, N. *Conduction in Non-Crystalline Materials*; Clarendon Press: Oxford, U.K., 1987; p 28.
(32) Tran, P.; Alavi, B.; Gruner, G. *Phys. Rev. Lett* **2000**, *85*, 1564.
(33) May, V.; Kühn, O. *Charge and Energy Transfer Dynamics in Molecular Systems: A Theoretical Introduction*; Wiley-VCH: Berlin, 2000.
(34) Bell, R. J.; Dean, P. *Discuss. Faraday Soc.* **1970**, *50*, 55. Fidder, H.; Knoester, J.; Wiersma, D. A. *J. Chem. Phys.* **1991**, *95*, 7880. Ludwig, H.; Runge, E.; Zimmermann, R. *Phys. Rev. B* **2003**, *67*, 205302.
(35) Levich, V. G.; Dogonadze, R. R. *Dokl. Akad. Nauk SSSR* **1959**, *124*, 123; **1960**, *133*, 158.
(36) Ulstrup, J. *Charge Transfer in Condensed Media*; Springer, Berlin, 1979.
(37) Kubo, R.; Toyozawa, Y. *Prog. Theor. Phys.* **1955**, *13*, 160.
(38) Marcus, R. A. *J. Chem. Phys.* **1956**, *24*, 966.
(39) Lax, M. *J. Chem. Phys.* **1952**, *20*, 1752.
(40) Rudolph, B. R.; Case, D. A. *Biopolymers* **1989**, *28*, 851.
(41) Treadway, C.; Fiebig, T. Private communication.
(42) Giacomoni, P. U.; Le Bret, M. *FEBS Lett.* **1973**, *29*, 227.
(43) A fragment of 22 sites was considered with G at site one, GGG at site $N + 2$, and A at the remaining sites.
(44) Voityuk, A. A.; Rösch, N.; Bixon, M.; Jortner, J. *J. Phys. Chem. B* **2000**, *104*, 9740.
(45) Troisi, A.; Orlandi, G. *Chem. Phys. Lett.* **2001**, *344*, 509.
(46) The range for the couplings obtained in ref 45 is due to slightly different equilibrium geometries for different systems with available crystallographic data.
(47) Hush, N. S.; Cheung, A. S. *Chem. Phys. Lett.* **1975**, *34*, 11.
(48) Seidel, C. A. M.; Schulz, A.; Sauer, M. H. M. *J. Phys. Chem.* **1996**, *100*, 5541.
(49) Our estimated energy gap, $\Delta_{AG} = 0.14$ eV, is smaller than the values of 0.2, 0.47, and 0.46 eV resulting from gas-phase measurements,[47] measurements in solution,[48] and semiempirical calculations[60] that were discussed in detail in Appendix F. One should note, however, that the energetic difference between G and the partially delocalized bridge states of A's is larger than this value because of the different solvation energies of the localized state at G and the partially delocalized bridge states.
(50) The present energetic gap between G and GGG of 0.2 eV may be compared with a wide variety of other values, such as the 0.68 eV estimated from earlier ab initio calculations (Sugiyama, H.; Saito, I. *J. Am. Chem. Soc.* **1996**, *118*, 7063) and of 0.13 eV estimated in recent semiempirical calculations.[60] Recent time-dependent experiments (Lewis F. D.; Liu, X.; Liu, J.; Hayes, R. T.; Wasielewski, M. R. *J. Am. Chem. Soc.* **2000**, *122*, 12037) gave a value of 0.08 eV for this energy gap.
(51) Segal, D.; Nitzan, A.; Ratner, M.; Davis, W. B. *J. Phys. Chem. B* **2000**, *104*, 2790.
(52) During the revision of this manuscript, a paper by Petrov et al. (Petrov, E. G.; Shevchenko, Ye. V.; May, V. *Chem. Phys.* **2003**, *288*, 269) was published with an identical phenomenological hopping constant as our eq 3. We would like to emphasize that our result was obtained independently and was presented in May 2002 at a meeting of the Electrochemical Society in Philadelphia, PA (U.S.A.), in May 2002 in a talk at Free University Berlin (Germany), and in November 2002 in talks at University of Nagoya, Kyoto University, and Tsukuba University (Japan).
(53) Zhang, W. M.; Meier, T.; Chernyak, V.; Mukamel, S. *J. Chem. Phys.* **1998**, *108*, 7763.
(54) Zhang, W. M.; Meier, T.; Chernyak, V.; Mukamel, S. *Philos. Trans. R. Soc. London* **1998**, *356*, 405.
(55) Knapp, E. W.; Fischer, S. F. *J. Chem. Phys.* **1988**, *90*, 354.
(56) Higai, S.; Sumi, H. *J. Phys. Soc. Jpn.* **1994**, *63*, 4489.
(57) Davis, W. B.; Hess, S.; Naydenova, I.; Haselsberger, R.; Ogrodnik, A.; Newton, M. D.; Michel-Beyerle, M.-E. *J. Am. Chem. Soc.* **2002**, *124*, 2422.
(58) The yield for short bridge lengths, where superexchange dominates, is calculated in Figures 4 and 5 to decrease with disorder. The origin of this effect lies in the back transfer $(GGG)^+ + G \rightarrow GGG + G^+$. The rate constant of the latter, for small energy gaps $\Delta E_{G,GGG}$ and small bridge lengths, becomes comparable to the trapping rate k_d and in this case leads to a distance-independent yield. With increasing disorder, the fraction of those DNAs with small $\Delta E_{G,GGG}$ increases, and therefore, the overall yield decreases for short bridge length.
(59) Jortner, J. Private communication.
(60) Voityuk, A. A.; Jortner, J.; Bixon, M.; Rösch, N. *Chem. Phys. Lett.* **2000**, *324*, 430.
(61) Lewis F. D.; Kalgutkar, R. S.; Wu, Y.; Liu, X.; Liu, J.; Hayes, R. T.; Miller, S. E.; Wasielewski, M. R. *J. Am. Chem. Soc.* **2000**, *122*, 12346.
(62) Cho, M.; Fleming, G. R. *Adv. Chem. Phys.* **1999**, *107*, 311.
(63) One possible source for different local hole energies of identical base pairs concerns the possible modulation of energies by counterions[32] (Barnett, R. B.; Cleveland, C. L.; Joy, A.; Landman, U.; Schuster, G. B. *Science* **2001**, *294*, 567) of the solution, which are attracted by the negatively charged sugar−phosphate backbone of DNA.
(64) Zwanzig, R. *Nonequilibrium Statistical Mechanics*; Oxford University Press: Oxford, U.K., 2001; p 104.
(65) Haken, H. *Quantum Field Theory of Solids: An Introduction*; North-Holland: New York, 1976.
(66) Chan, C. K. *J. Chem. Phys.* **1984**, *81*, 1614.
(67) Marcus, R. A. *J. Phys. Chem. B* **1998**, *102*, 10071.
(68) Tanaka, S.; Sengoku, Y. *Phys. Rev. E* **2003**, *68*, 031905.
(69) Risser, S. M.; Beratan, D. N.; Meade, T. J. *J. Am. Chem. Soc.* **1993**, *115*, 2508.